Supplement

Supplemental Methods

Bioinformatics and Statistical Analysis of Gene Expression Profiles. We compiled 6 archived gene expression profiling datasets that measured expression from pediatric B-precursor ALL (BPL) patients and were generated using the Human Genome U133 Plus 2.0 Array platform from Affymetrix (GSE11877, N=207; GSE13159 N=823; GSE13351 N=107; GSE18497, N=82, GSE28460, N=98; GSE7440, N=99; Total N=1416). To enable comparison of samples across studies, a normalization procedure was performed that merged the raw data from the 6 datasets (CEL files). Perfect Match (PM) signal values for probesets were extracted utilizing raw CEL files matched with probe identifiers obtained from the Affymetrix-provided CDF files (HG-U133_Plus _ 2.cdf) implemented by Aroma Affymetrix statistical packages run in an R-studio environment (Version 0.97.551, R-studio Inc., running with R 3.01). The PM signals were quantified using a Robust Multiarray Analysis (RMA) in a 3-step process, including RMA background correction, quantile normalization, and summarization by median polish of probes in each probeset across 1416 samples (RMA method adapted in Aroma Affymetrix). In order to elucidate the genetic biomarkers for therapeutic TRAIL sensitivity in primary leukemia cells from high-risk BPL patients, we focused our analysis on publicly available archived gene expression profiles of primary leukemia cells from BCR-ABL$^+$ BPL patients (123 samples from GSE13159 and GSE13351), E2A-PBX1$^+$ BPL patients (61 samples from GSE11877, GSE13159 and GSE13351), patients with multi-lineage leukemia (MLL) gene rearrangements (MLL-R$^+$) (95 samples from GSE11877, GSE13159 and GSE13351) in side by side comparison with gene expression profiles of primary leukemia cells that were negative for each of these high-risk molecular markers (N=595 from GSE11877, GSE13159 and GSE13351). An archived dataset on gene expression profiles of primary leukemia

cells in matched-pair bone marrow specimens obtained at initial diagnosis and 1st relapse from 49 pediatric patients with BPL (GSE28460) was also interrogated. Probesets for the 71-gene TRAIL sensitivity signature were obtained from the Affymetrix NetAffx™ Analysis Center (http://www.affymetrix.com/analysis/index.affx); 146 probesets for 68 of these 71 genes were represented on the Human Genome U133 Plus 2.0 Array. We also examined the expression levels for 9 TRAIL receptor-linked death pathway genes (31 probesets for CASP10, CASP16, CASP3, CASP7, CASP8, CASP9, CFLAR, FADD and TRADD), the peptidyl O-glycosyltransferase GALNT14 gene, the CD19 gene, and TRAIL-receptor genes (17 probesets for CD19, TNFRSF10A, TNFRSF10B, TNFRSF10C, TNFRSF10D, TNFRSF11B) in these primary BPL cells.

We constructed two mixed models of analysis of variance (ANOVA) (one for the comparison of initial versus relapse clones in matched-pair specimens and one comparing primary leukemia cells in high-risk BPL patient subgroups) utilizing RMA-normalized gene expression levels to identify significant differences revealed by probesets for the transcripts encoded by these genes. We then used a supervised approach with planned linear contrasts to assess significant effect sizes in probeset-specific and gene set-specific comparisons. Two fixed factors (patient subgroups and the Affymetrix probeset ID), one interaction term (Patient sub-group x Affymetrix probeset ID) and one random factor (GSM number from the GEO database for each sample) were employed in the models. The random effect controlled for multiple measurements taken from each patient and modeled this as a separate variance component using the restricted maximum likelihood (REML) method. The least squares method was used to fit the parameters for the mixed models and the parameters were utilized to generate prediction equations and best fit lines visualized by plotting the leverage graphs using standard coding procedures. We examined the distribution of the residuals in the models for equal dispersion around the line of best fit and to assess the patterns in the residuals. Effect sizes from differences between least square mean estimates were used in the design of planned linear contrasts to determine the significance of the observed differences in

gene expression levels. Two-tailed P-values were calculated in the JMP software [SAS, Cary, NC]) and P-values <0.05 were deemed significant. The standard error estimates used for testing differences between group means were obtained from the residuals of the linear fit for all the data. A two-way hierarchical clustering technique was utilized to visualize similar expression of probesets and patient samples using $\log_2$ transformed RMA expression values mean centered to control samples in the comparisons. Pair-wise Pearson product-moment correlations were performed between DR4, DR5, CD10, CD19, and CD34 expression levels in primary leukemia cells obtained from diagnostic bone marrow specimens of 21 high-risk BPL patients (JMP v10, SAS, Cary, NC). Least squares regression analysis was utilized to determine the fraction of variation explained by the Pearson correlation (square of the correlation coefficient, R-squared) and significance of the association was tested against zero correlation using the F-test for regression. P values less than 0.05 were deemed significant.

Recombinant Human CD19L-sTRAIL Fusion Protein. In order to construct an expression cassette for a recombinant human CD19 Ligand (CD19L)-soluble TRAIL (sTRAIL) fusion protein, we designed and implemented a stepwise molecular cloning strategy using the commercially available pFUSE-hIgG1-Fc2 plasmid (Invivogen, CA) as the backbone vector. As a first step, the 1.5-Kb protein-coding fragment of the CD19L cDNA was amplified by PCR from our recently published pFASTBAC-rhCD19L construct (1) using the Phusion High-Fidelity PCR kit (NEBs E0553L) (Primers: Forward/Reverse: 5'- CCAGGGAATTCCTATATGAGCATGACAGA-3'/5'-CCGGAGATCTAGTAAGGTACAGTGCTTT). This CD19L cDNA fragment was inserted in-frame downstream of a 60-bp human IL2 signal sequence (ss) of the backbone vector through two unique EcoRI and BglII restriction sites using the Quickligase™ Kit (NEBs) following the manufacturer's recommendations to generate a pFUSE-CD19L-hIgG1-Fc2 plasmid (CD19L-hIgG1-Fc PL). The mCH1 linker previously used in the generation of biologically active sTRAIL fusion proteins (2) is comprised of a 19-residues segment of the IgG1-CH1 domain

(AAAEFAKTTAPSVYPLEPV) followed by two amino acids from the XhoI restriction site (LE) and a five amino acids flexible hydrophilic region (SSGSG). A synthetic complementary duplex derived from reverse translation of the amino acid sequence of the mCH1 linker with BglII and NheI restriction sites at the 5' and 3' ends, respectively, was ligated in-frame to the 3' end of CD19L cDNA through the BglII and NheI sites. As a result, the IgG1-Fc fragment was displaced and a pFUSE-CD19L-mCH1 linker cassette was generated. A fragment encoding amino acids 114 to 281 of the TRAIL protein was amplified from the commercially available TRAIL cDNA (pCMV6AC-TRAIL vector SC#321920, Origene, CA, USA) by PCR using the forward primer 5'-GCTAGCAGTGAGAGAAAGAGGTCCTCAG-3' and the reverse primer 5'-GCTAGCTTAGCCAACTAAAAAGGCCCCAA-3'. The soluble TRAIL (sTRAIL) cDNA (~0.5 kb) fragment obtained by PCR was ligated to the 3' end of the CD19L-Linker cassette through a unique NheI site and the pFUSE-CD19L-mCH1-sTRAIL fusion construct was successfully assembled (Accession number: LN651283, European Nucleotide Archive). pFUSE-CD19L-mCH1-sTRAIL was expressed in the human embryonic kidney cell line Hek293T. Cells were grown in a 15 cm-plate containing DMEM medium supplemented with 10% FBS at 37^{o}C, 5% CO_2. When cell growth reached 90% confluency, transfection of the cells with the CD19L-sTRAIL expression cassette (33 μg DNA/plate) was carried out using the polymeric reagent polyethylenimine (PEI, Sigma, Co#: 408727). Hek293T cells were transfected with pFUSE-CD19L-mCH1-sTRAIL expression construct or empty vector (VC). To confirm expression of the fusion transcript, total RNA was extracted from transfected cells after 24 hrs. One-step RT-PCR was performed using the sTRAIL cloning primer set (F: 5' AGAGAAAGAGGTCCTCAG, R: 5' TTGGGGCCTTTTTAGTTGGCTAA). A 0.5kb PCR product was shown only in the pFUSE-CD19L-mCH1-sTRAIL transfected cells, but not in the VC transfected cells. For CD19L-sTRAIL fusion protein production, Hek293T cells were harvested 7-8 days after transfection with the pFUSE-CD19L-mCH1-sTRAIL expression construct, pelleted and lysed for one hour on ice in 50 mM Tris-base (Fisher Scientific BP152-500), pH 7.4, 150 mM NaCl, 1 mM EDTA supplemented with 1%

(v/v) Triton X-100 and a cocktail of protease inhibitors [2 mM AEBSF (4-(2-Aminoethyl) benzenesulfonyl fluoride hydrochloride), 1 µM phosphoramidon disodium salt, 130 µM bestatin, 14 µM E-64 (N- (trans-Epoxysuccinyl)-L-leucine 4-guanidinobutylamide), 1 µM Leupeptin, 0.2 µM Aprotinin, 10 µM pepstatin A] according to the manufacturer's instructions (SigmaFAST Protease Inhibitor Cocktail, Sigma Cat. # S8830)]. After one hour of mixing, the lysate was spun at high speed for 10 minutes in a microfuge to remove cell debris. The supernatant was subsequently concentrated using Centriprep Centrifugal Filter Units (15 mL) with a 50-kDa cut-off Ultracel YM-50 membrane (EMD Millipore, Billerica, MA). The concentrated samples were put through a 4 ml Pierce Detergent Removal Spin column to remove the Triton X-100 detergent. Eluted material from these columns was combined and dialyzed against 50 mM borate buffer, pH 8.8, using Pierce Slide-a-Lyzer dialysis cassettes (Thermo Fisher Scientific), in preparation for the ion exchange step. Pierce Strong Anion Exchange (AIE) mini spin columns (Thermo Fisher Scientific) were equilibrated in 50 mM borate, pH 8.8, and 0.4 mL of the dialyzed CD19L-sTRAIL lysate was applied to each mini spin column. After centrifugation, each mini column was washed with 0.6 mL total (2 x 0.3 mL) of 50 mM borate, pH 8.8, to remove unbound material. Elution of bound proteins was then accomplished in a step-wise fashion using a total of 0.6 mL (2 x 0.3 mL for each step) of 50 mM borate, pH 8.8, containing 0.1 M NaCl, 0.25 M NaCl, 0.5 M NaCl, or 0.75 M NaCl. Most of the CD19L-sTRAIL was found in the 0.1 M NaCl fraction. This fraction was then concentrated and applied to a 1.5 x 50 cm S-200 HR Sephacryl size exclusion (SE) column in PBS at a flow rate of 0.1 ml/min. The absorbance at 280 nm was followed and CD19L-sTRAIL- containing fractions were identified using an anti-TRAIL dot blot procedure. The peak samples were pooled and concentrated using the 50-kDa cut-off devices as described above. SDS-PAGE of purified CD19L-sTRAIL (30 µg of the post-AIE sample and 5 µg of the post-AIE+SE samples) was carried out under nonreducing conditions using Bio-Rad's 4-20% tris/glycine SDS gradient mini gels. Electrophoresis was performed at 200V, constant voltage, and gels were subsequently stained using Bio-Rad's Bio-Safe Coomassie Blue stain. Precision Plus Protein Kaleidoscope

Standards #161-0375 (Bio-Rad, Life Science Research, Hercules, CA) containing a mixture of 10 recombinant proteins (10-250 kDa) were used for molecular weight sizing on SDS-PAGE gels. The gel was scanned with Copystar Image 2000 scanner at a resolution of 600 dpi. The jpeg image was then uploaded on the ImageJ software (NIH, http://imagej.nih.gov/ij/docs/) where the bands were quantified. The image was converted into an 8 bit gray scale image and the lane of interest was selected for densitometric analysis. The sTRAIL and CD19L domains of the fusion protein were detected by Western blot analysis using standard procedures (1,3,4). We used a solid phase sandwich ELISA, in which a mouse IgG1 monoclonal antibody specific for human TRAIL was used to precoat the microplate wells, to measure the sTRAIL-based molar concentrations of the CD19L-sTRAIL samples. This monoclonal antibody was generated against *E. coli*-derived recombinant human TRAIL (Val114 – Gly281) (Human TRAIL/TNFSF10, catalog #DTRL00, R & D Systems). A recombinant human sTRAIL 19.6 kDa protein (PeproTech, Catalog Number: 310-04) expressed in *E. coli* was also used as a standard for the kit. This sTRAIL standard contains 168 amino acids consisting of the TNF homologous portion of the extracellular domain of full-length TRAIL.

NHS-Fluorescein (NHSF) (5/6-carboxyfluorescein succinimidyl ester; CAS # 76608-16-7; Excitation wavelength: 494 nm, Emission wavelenth: 518 nm – both identical to the same parameters for FITC; Product # 46410, Thermo Scientific, Waltham, MA) was used for fluorescent labeling of CD19L-sTRAIL via its primary amines according to the manufacturer's recommendations. Compared to FITC, the NHS-ester derivative has greater specificity toward primary amines in the presence of other nucleophiles and results in a more stable amide linkage following labeling. NHS-Fluorescein was dissolved in DMSO just prior to use and added to the CD19L-sTRAIL protein in PBS at an approximate molar ratio of 100:1, NHS-Fluorescein: protein. Incubation was carried out by rotating the sample for 1 ½ hrs at 35^{o}C in a controlled temperature chamber protected from light. Unreacted NHS-Fluorescein and small molecular weight reaction products were removed by passing the sample through a Zeba desalting spin column (Thermo

Scientific) in PBS and the NHS-Fluorescein labeled CD19L-sTRAIL protein was stored at 4^{o}C for testing. sTRAIL was also labeled with NHSF to compare its binding to the surface of BPL cells to the binding of CD19L-sTRAIL.

Recombinant human CD19L-hIgG1-Fc fusion protein. We used an Fc fusion protein of CD19L in some blocking experiments to confirm that the binding of the FITC-labeled CD19L-sTRAIL fusion protein to leukemia cells is mediated via its CD19L domain. The full-length cDNA of CD19L was amplified by PCR with forward primer 5'-CCAGGGAATTCCTATATGAGCATGACAGA-3' and reverse primer 5'-CCGGAGATCTAGTAAGGTACAGTGCTTT-3'. The correct amplicon (1.5-Kb) was ligated to the EcoRI and the BglII sites at the 5'-end of the Fc fragment of the pFUSE-hIgG1-Fc2 plasmid. The CD19L-Fc fusion protein was expressed in Hek293T cells and then purified using the Affi-Gel Protein A MAPS II Kit from Bio-Rad Laboratories. Since the CD19L-Fc protein contains an Fc region, it was purified on the Affi-Gel Protein A support. The kit contains a binding buffer (pH 8.8-9.2) and an elution buffer at a pH of 2.8 – 3.0. The eluted protein was immediately neutralized and put through a 'desalting' column to equilibrate it in PBS, pH 7.4, before use.

Recombinant human CD19L, CD19-ECD, and CD19-ICD Proteins. The 1.5-Kb CD19L cDNA fragment including its protein coding segment was cloned into the NcoI/KpnI site of the 4.9-Kb pFastBacHT (PFBH) donor vector (Life Technologies) containing a 6x-histidine (6xHis) tag to construct a 6.5-Kb recombinant PFBH-CD19L plasmid (1). PFBH-CD19L was used to generate a recombinant baculovirus by site-specific transposition in *Escherichia* (*E*.) *coli* DH10Bac competent cells (Life Technologies), which harbor a baculovirus shuttle vector (bacmid), bMON14272 with a mini-attTn7 target site for site-specific transposition using previously reported procedures (1). The bacterial colonies containing recombinant bacmids were identified by disruption of the lacZ gene. High molecular weight miniprep DNA was prepared from selected *E.coli* clones containing recombinant bacmid and transfected into Sf21 cells using the Cellfectin reagent (Life

Technologies) as previously described (1). Histidine-tagged recombinant CD19L was produced in Sf21 cells and purified via multiple chromatography steps using a Nickel-chelation column (Pharmacia), Sepharose Q HP26/10 ion exchange column (column volume 50 ml; Amersham Pharmacia Biotech), and size exclusion chromatography on a Superdex 200 HR 10/30 column (Pharmacia) as previously published (1). The cDNA encoding the extracellular domain (AA 1-273) of human CD19 ($CD19^{ECD}$) was cloned into the pFastBac1 (PFB) donor vector (Life Technologies), as previously published (1). The resulting pFast-bac-$CD19^{ECD}$ recombinant plasmid (PFB-$CD19^{ECD}$) was then used to generate the recombinant baculovirus by site-specific transposition in *Escherichia coli* DH10Bac competent cells (Life Technologies), which harbor a baculovirus shuttle vector (bacmid), bMON14272 with a mini-attTn7 target site for site-specific transposition using previously reported procedures (1). PFB-$CD19^{ECD}$ was inoculated into SF21 cells, and the cells were used 48 hours later for pull-down and immunoblotting experiments. Likewise, the cDNA encoding full-length CD19 as well as cDNA encoding the intracellular domain (ICD) (AA 300-540) of human CD19 were cloned into the pFastBac1 vector and recombinant full-length CD19 and $CD19^{ICD}$ were produced in the baculovirus expression system, as reported (1).

Standard chemotherapy drugs. We used the standard chemotherapy drugs commonly used in BPL therapy, including Vincristine (Lot #: X067139A; Manufacturer: Hospira Inc Lake Forest, IL), Doxorubicin (Adriamycin; Lot #: 2005342; Manufacturer: Ben Venue Labs Inc Bedford, OH), PEG-Asparaginase (Oncospar; Lot #: 0009A; Manufacturer: Enzon Pharmaceuticals Inc Bridgewater, NJ); as well as Dexamethasone (Cat. #: D9184-100MG; Sigma Saint Louis, MO) as controls. The chemotherapy drugs were obtained from the Pharmacy of the Children's Hospital Los Angeles.

Immunophenotyping, Immunofluorescence Microscopy, Immunoprecipitations, Western Blot Analyses, Apoptosis Assays and Colony Assays. Immunophenotyping (3), confocal imaging (4,5), immunoblotting using the ECL detection system (Amersham Pharmacia Biotech) (4-

7) and apoptosis assays (6,8) were performed, as described in detail in previous publications. For analysis of the immunoreactivity of CD19L-sTRAIL with $CD19^+$ ALL-1 ($BCR\text{-}ABL^+$ B-precursor ALL cell line) and $CD19^-$ Hek293T cells, we used NHS-Fluorescein labeled CD19L-sTRAIL protein (10 pM). In some experiments, a 100-fold molar excess of CD19L-hIgG1-Fc fusion protein (1 nM) was used to block the binding of NHS-Fluorescein labeled CD19L-sTRAIL protein to $CD19^+$ ALL-1 cells. In other experiments, a 50-fold molar excess of sTRAIL was used the block the binding of NHS-Fluorescein-labeled CD19L-sTRAIL to ALL-1 cells. In flow cytometric immunophenotyping of primary leukemia cells, we used FITC-labeled anti-DR4 mouse MoAb (Cat# ab59047, Abcam, Cambridge, MA), PE-labeled anti-DR5 mouse MoAb (Cat#FAB6311P, R&D Systems, Minneapolis, MN), APC-labeled anti-CD10 mouse MoAb (Cat#340923, BD Biosciences), PE-labeled anti-CD10 mouse MoAb (Cat#55375, BD Biosciences, San Jose, CA), Alexa Fluor 700-labeled anti-CD19 mouse MoAb (Cat #557921, BD Biosciences, San Jose, CA), and PerCP-Cy5.5 labeled anti-CD34 mouse MoAb (Cat#347203, BD Biosciences, San Jose, CA). Controls included unstained cells as well as cells that were stained with a cocktail of control mouse IgG labeled with PE, FITC, APC, AF700, and PerCP-Cy5.5. The labeled cells were analyzed on a LSR II flow cytometer (Becton Dickinson, Lakes, NJ). Percent positivity for each antigen/antigen pair was Arc Sine transformed to enable clustering of the expression data. One-way agglomerative hierarchical clustering of the flow cytometry data was performed to depict the groups of leukemia cells that exhibited similar profiles.

In confocal microscopy experiments, slides were imaged using the PerkinElmer Spinning Disc Confocal Microscope and the PerkinElmer UltraView ERS software (Shelton, CT) or the Velocity V5.4 imaging software (PerkinElmer, Shelton, CT). We used standard flow cytometric quantitative apoptosis assays (6) to compare the anti-leukemic activity of CD19L-sTRAIL, sTRAIL, CD19L, ionizing radiation, or standard chemotherapy drugs against primary leukemia cells from patients with BPL as well as ALL xenograft cells derived from B-precursor ALL patients. Exposure of

phosphatidylserine on the outer leaflet of the target leukemia/lymphoma cell membrane was measured using FITC-conjugated Annexin-V, the natural ligand of phosphatidylserine. Apoptotic ALL cells were labeled with PI and Annexin-V-FITC using the Annexin V-FITC apoptosis detection kit (Sigma, Catalog # APOAF-50TST) according to the manufacturer's recommendations. In other experiments, we used an alternative assay system, in which cells were stained with a PE-labeled anti-CD19 MoAb and FITC-conjugated Annexin-V (8). The labeled cells were analyzed on a LSR II flow cytometer (Becton Dickinson, Lakes, NJ).

The anti-leukemic potency of various treatments was documented by comparing the numbers of residual viable lymphoid cells in the 24h or 48h cultures of untreated control cells vs. 24 h or 48h cultures of cells exposed to the test treatments. Specifically, the number of viable cells was determined by first determining in each sample the number of lymphoid cells remaining in the P1 lymphoid window of the FSC/SSC light scatter plots using the formula: N(P1) = 10,000 (i.e. total number of cells analyzed) x % of cells in P1. Then, we determined the % of viable cells in the P1-window as the % of Annexin V-FITC$^-$PI$^-$ cells in the left lower quadrant of the Annexin V-FITC vs. PI fluorescence intensity dot plots. The number of viable lymphoid cells (N[viable]) was then determined using the formula: N(P1) x % Viable Cells in P1/100. The percent apoptosis (%A) was calculated using the formula: 100- N[viable] for Test sample] / N[viable for Control sample] x100. We constructed a general linear model with one factor that identified treatment effect for either primary leukemia cells from BPL patients or BPL xenograft cells for the analysis of the apoptosis data. The statistical model included a fixed effect ("Treatment") and a random effect ("Case") that controlled for multiple measurements taken from a BPL xenograft case or primary BPL cells. The least squares method was used to fit the parameters for the general linear model and these parameters were utilized to generate prediction equations and best-fit lines were visualized by plotting leverage graphs using standard coding procedures. We examined the distribution of the residuals of the model for equal dispersion around the line of best fit to assess the effect of the

boundary values of 0 and 100 on the model. Effect sizes from differences between treatment least square mean estimates were used in the design of planned linear contrasts to determine significant effects (two-tailed $p<0.05$ deemed significant calculated in JMP software [SAS, Cary, NC]). The standard error estimate (Root Mean square Error term in the model) used for testing differences between group means was obtained from the residuals of the linear fit for all the data and this minimized the effect of skewed standard deviation estimates from measurements close to the boundary values. To compare group means between 2 treatments within a single level of a factor, the linear contrast utilized the standard error derived from the model and the comparison group means were coded with linear parameter values of 1 and -1 to calculate effect size between the 2 treatments. In comparisons that tested differences from pooling the mean from combining treatment groups within a single level of a factor, the comparison group means were coded such that the combination of linear parameters to be jointly tested was summed to zero for the linear contrast. Significant treatment effects were determined using a linear contrast model defined by one fixed factor for treatment dose and one random factor to control for multiple measurements taken from each "case". Two separate models were constructed for primary BPL cells and BPL xenograft cells. Linear combination of parameters setting the 2Gy radiation group to "1" and each of the dose concentrations to "-1" measured the effect size at each dose. For documentation of TRAIL-R linked death pathway activation in the CD19L-sTRAIL treated $CD19^+$ BPL cell line ALL-1 by Western blot analysis, we used the following antibodies from the Cleaved Caspase Antibody Sampler Kit from Cell Signaling Technology (Cat# 9929, Danvers, MA): (1) Rabbit MoAb 5A1E recognizing the 17.2-kDa cleaved caspase-3 (CASP3) (Asp175) protein (Product#9664), (2) Rabbit MoAb product #9761 recognizing the 18-kDa cleaved caspase 6 (CASP6) (Asp162) protein, (3) Rabbit MoAb D2D4 (Product #7237) recognizing the 35-kDa Caspase 9 (CASP9) (Asp330) protein, and (4) Rabbit MoAb D64E10 (Product #5625) recognizing the 89-kDa cleaved PARP (Asp214) protein. We used a rabbit polyclonal anti-α/β-Actin antibody (Cat#A5060, Sigma-Aldrich, St.Louis, MO) and a mouse monoclonal anti-α-Tubulin antibody (Sigma Cat# T6199; Sigma-

Aldrich, St.Louis, MO). HRP-linked goat anti-mouse IgG (Cat# sc-2005, Santra Cruz Biotechnology (Santa Cruz, CA) served as a secondary antibody for primary mouse antibodies and HRP-linked goat anti-rabbit IgG (antibody product #7074; Sigma-Aldrich, St.Louis, MO) served as the secondary antibody for primary rabbit antibodies. We also examined the effects of the selective CASP8 inhibitor Z-IETD-FMK (Cat. #1064-20C, Biovision, Inc.; Milpitas, CA) (25 μM) and CASP9 inhibitor Z-LEHD-FMK (Cat. # 1149-1; Biovision, Inc.; Milpitas, CA) (20 μM) on the TRAIL-R linked death pathway activation in ALL-1 cells treated with 840 fM CD19L-sTRAIL for 2 h. The inhibitors were added to the cultures 15 min prior to addition of CD19L-sTRAIL. In other experiments of PARP activation by CD19L-sTRAIL, 1 nM sTRAIL was used in side-by-side comparison to or in combination with 20 pM CD19L-sTRAIL. In 2 experiments, we used in vitro colony assays to examine the effects of 2.1 pM CD19L-sTRAIL on the clonogenic survival of human BPL cell line ALL-1 vs. non-leukemic pro-B cell line FL8.2 (3) and mature B-cell line BCL-1 (4). Cells were treated with 2.1 pM CD19L-sTRAIL for 24h and then assayed in duplicate for colony formation in semi-solid methylcellulose cultures. Specifically, after treatment, cells ($0.3x10^6$ cells/mL) were suspended in RPMI supplemented with 0.9% methylcellulose, 30% fetal bovine serum, and 2 mM L-glutamine. Controls included untreated cells. Duplicate 1 mL samples containing $0.3x10^6$ cells/sample were cultured in 35 mm Petri dishes for 7 d at 37^oC in a humidified 5% CO_2 atmosphere. On d7, colonies containing ≥20 cells were counted using an inverted Nikon Eclipse TS100 microscope.

Leukemia cells. Primary leukemia cells isolated from bone marrow (N=27) or peripheral blood (N=6) specimens of 34 patients with BPL (New Diagnosis = 31; Relapse = 3) and 21 clones derived from spleen specimens of xenografted 21 NOD/SCID mice inoculated with leukemia cells from 11 BPL xenograft cases were used in the described experiments. Of these 21 clones, 3 were derived from Xeno case#7, 5 were derived from Xeno Case#8, 2 were from Xeno Case#10, and 4 were from Xeno Case #11. The remaining 7 clones were from Xeno Case #'s 1, 2, 3, 4, 5, 6, and

9. The 11 xenograft cases were established using primary cells from 8 newly diagnosed and 3 relapsed pediatric BPL patients. The secondary use of leukemic cells for subsequent molecular studies did not meet the definition of human subject research per 45 CFR 46.102 (d and f) since it did not include identifiable private information, and it was approved by the IRB (CCI) at the Children's Hospital Los Angeles (CHLA) and the Memorial Care Health System Institutional Review Board at Miller Children's Hospital, Long Beach, CA. We further used the BPL cell line ALL-1 (Ph^+ adult BPL), Burkitt's leukemia (B-ALL)/lymphoma cell line RAJI as targets. In addition, we used the EBV-transformed human pro-B cell line FL8.2 (3) and the EBV-transformed mature human B-cell line BCL-1 (4) to determine the effects of CD19L-sTRAIL on non-leukemic human B-cell precursors and B-cells.

Irradiation of cells and mice. NOD/SCID mice were irradiated with single dose TBI (2 Gy delivered at 106 cGy/min) using a self-shielded Cs-137 irradiator (Mark I Irradiator-68A, JL Sheperd & Associates, San Fernando, CA), as previously reported (6). Cells were also irradiated with 200 cGy γ-rays in a single exposure using the Mark I Cs-137 irradiator (6). Radiation resistance was defined as a surviving faction at 2 Gy (SF2) of ≥50%. All personnel using the irradiator completed the "Radiation Safety Training for Operators of Cs-137 Irradiators" and completed a formal operational training in the safe and proper operation of the irradiator in compliance with the radiation safety procedures of the Children's Hospital Los Angeles as directed by the CHLA Radiation Safety Officer.

Preclinical toxicity studies of CD19L-sTRAIL in mice. We examined the toxicity of CD19L-sTRAIL in xenografted NOD/SCID mice as well as healthy non-leukemic C57BL/6 mice using published procedures (6, 9). The research in female NOD/SCID mice was conducted according to Institutional Animal Care and Use Committee (IACUC) Protocol #280-09 that was approved by the IACUC of CHLA on 11-24-2009 and its 3-year renewal 280-12 that was approved on 7-10-2012.

The research in C57/BL/6 mice was conducted according to IACUC Protocol #293-13 that was approved by the IACUC of CHLA on 6-13-2013. All animal care procedures conformed to the Guide for the Care and Use of Laboratory Animals (National Research Council, National Academy Press, Washington DC 1996, USA). Trained personnel of the AAALAC-approved Saban Institute Animal Care Facility (ACF) provided care for animals. Female C57/BL/6 mice (6 mice/group) were treated with a single intravenous bolus dose of CD19L-sTRAIL at 32 fmol/kg, 320 fmol/kg, 640 fmol/kg, or 3.2 pmol/kg. The control group (N=6) included untreated mice. Mice were allowed free access to autoclaved standard pellet food and tap water throughout the experiments and monitored daily for signs of morbidity and mortality. Mice were electively sacrificed at 28 days by CO_2 inhalation to determine the toxicity of CD19L-sTRAIL by examining their blood chemistry profiles, blood counts, and evaluating multiple organs for the presence of toxic lesions. Blood was collected by cardiac puncture after euthanasia. The blood chemistry profiles were examined using an Olympus AU5400 Chemical Analyzer (Sacramento, CA). Blood counts (red blood cells [RBC], white blood cells [WBC] and platelets [Plt]) were determined using a Bayer Advia 120 blood analyzer (San Diego, CA). The chemistry tests performed on the collected serum samples were: Albumin, Alanine Aminotransferase (ALT), Amylase, Lipase, Blood Urea Nitrogen (BUN), Creatinine, Total Bilirubin, and Total Protein. Bone marrow function was assessed by complete blood counts (CBC) as well as microscopic bone marrow examinations. Liver toxicity was assessed with measurements of serum levels of ALT, Alkaline Phosphatase (Alk.Ptase), LDH and Total Bilirubin. Pancreas toxicity was assessed with measurements of serum amylase and lipase levels. Renal toxicity was assessed with measurements of serum creatinine and BUN levels. Albumin and glucose levels were also measured. Two-sample Student's T-tests (degrees of freedom adjusted for unequal variances) were performed to assess the significance of the differences in spleen counts, CBC or Blood Chemistry between treatment groups. P-values of less than 0.05 were deemed significant and not corrected for multiple comparisons if the false discovery rate was less than 5% for the number of comparisons that were performed across all the pairwise

treatment groups and CBC/Blood Chemistry measurements. All mice underwent routine necropsy. At the time of necropsy, 19 different tissues (bone, bone marrow, brain, spinal cord, uterus, ovary, heart, thyroid gland, large intestine, small intestine, kidney, liver, lymph node, lungs, pancreas, peripheral nerve, skeletal muscle, thymus, urinary bladder) were collected within 15 min after sacrifice. Organs were preserved in 10% neutral phosphate buffered formalin, and processed for histologic sectioning. For histopathologic studies, formalin fixed tissues were dehydrated and embedded in paraffin by routine methods. Glass slides with affixed 4-5 micron tissue sections were prepared and stained with Hemotoxylin and Eosin (H&E). In addition, the spleens were removed, measured, and nucleated spleen cell counts were determined. Similar studies, including blood tests and histopathologic examinations were performed in xenografted NOD/SCID mice that were electively sacrificed when control mice developed leukemia-associated morbidity.

Pharmacokinetic Studies. In pharmacokinetic (PK) studies in C57BL/6 mice, CD19L-sTRAIL was injected as a single 2.0 pmol/kg iv bolus dose. For side-by-side comparison, separate groups of mice were injected with sTRAIL as a single 6.2 pmol/kg iv bolus dose. C57BL/6 mice (6-8 weeks of age, female) were obtained from the Jackson Laboratory (Sacramento, CA). In PK studies in NOD/SCID mice, CD19L-sTRAIL was injected as a single 2.0 pmol/kg iv bolus dose. The research was conducted according to Institutional Animal Care and Use Committee (IACUC) Protocols #293-10 and #280-12. All animal care procedures conformed to the Guide for the Care and Use of Laboratory Animals (National Research Council, National Academy Press, Washington DC 1996, USA). Trained personnel of the AAALAC-approved Saban Institute Animal Care Facility (ACF) provided care for the animals. Groups of mice were electively sacrificed at the indicated time points by CO_2 inhalation and blood was collected by cardiac puncture after euthanasia. We used a solid-phase ELISA kit (Quantikine ELISA Human TRAIL/TNFSF10 Immunoassay, Cat #DTRL00, R & D Systems, Minneapolis, MN) that employs an anti-TRAIL mouse MoAb to measure the plasma concentrations of sTRAIL and CD19L-sTRAIL at the indicated time points

after administration of an iv bolus dose of sTRAIL (6.2 pmol/kg) and CD19L-sTRAIL (2.0 pmol/kg), respectively. The PK modeling and PK parameter estimations were carried out by non-linear fitting of the plasma concentration vs. time profiles using the JMP 10 Software (SAS, Cary, NC) (6). An appropriate PK model was chosen on the basis of lowest sum of weighted squared residuals, lowest Akaike's Information Criterion value, lowest SE of the fitted parameters, and dispersion of the residuals (6, 9). The Y-intercept of plasma concentration-time profile determined the C_{max}. Definite analytic integrals from zero to 100 h were derived to calculate the Area Under the Curve ($AUC_{0\text{-}100h}$) for the 3 parameter exponential equation that best fitted the composite data points for CD19L-sTRAIL elimination and the single exponential equation that best fitted the sTRAIL elimination. To determine the Area Under the Moment Curve ($AUMC_{0\text{-}100h}$), definite integrals from the 0 h to 100 h time points were solved for the first moment exponential curves (CD19L-sTRAIL x Time versus Time for C57BL/6 and NOD/SCID mice) and sTRAIL (sTRAIL x Time versus Time for C57BL/6 mice). The Mean Residence time (MRT) was calculated by dividing the AUMC by AUC for each curve. On the assumption that the plasma elimination rate is the sum of first order processes, the plasma half life was calculated using the relationship defined by Plasma half life = 0.693 x MRT. We also performed specific comparisons of the plasma concentrations of sTRAIL vs. CD19L-sTRAIL at each time-point using a Planned Linear Contrast model for log10 transformed values and in this model values below zero were floored at a value of 1. The statistical model included two fixed effects ("Time" and "Formulation") and an interaction term (Time x Formulation). The least squares method was used to fit the parameters for the General Linear Model and these parameters were utilized to generate prediction equations and best fit lines visualized by plotting leverage graphs using standard coding procedures. We examined the distribution of the residuals of the model for equal dispersion around the line of best fit. Effect sizes were calculated from differences between the least square mean estimates of the respective plasma concentrations for sTRAIL and CD19L-sTRAIL (coded 1 and -1 in the specified contrasts). The effect sizes were used in the design of planned linear contrasts in order to

determine the significance of the observed differences in plasma concentrations at the indicated time points. The differences were deemed significant for two-tailed P-values <0.05 in the JMP software (SAS, Cary, NC). The standard error estimates (Root Mean Square error term in the model) used for testing differences between group means were obtained from the residuals of the linear fit for the cumulative dataset and this minimized the effect of skewed standard deviation estimates from floored concentration values.

NOD/SCID Mouse Xenograft Model of Human B-Precursor ALL. The anti-leukemic activity of CD19L-sTRAIL was studied in a NOD/SCID mouse model of human B-precursor ALL (6). NOD/SCID mice (NOD.CB17-*Prkdc*^{scid}/J; 4-6 weeks of age at the time of purchase, female) were obtained from the Jackson Laboratory (Sacramento, CA). The research was conducted according to Institutional Animal Care and Use Committee (IACUC) Protocol #280-09 that was approved by the IACUC of CHLA on 11-24-2009 and its 3-year renewal 280-12 that was approved on 7-10-2012. All animal care procedures conformed to the Guide for the Care and Use of Laboratory Animals (National Research Council, National Academy Press, Washington DC 1996, USA). The specific pathogen-free (SPF) environment for immunodeficient NOD/SCID mice was ensured by the use of Micro-Isolator cages, which were autoclaved, complete with rodent chow and hardwood Sani-Chips for bedding. Water was provided ad libidum and was also autoclaved as well as supplemented with Bactrim/Septra (0.89 mg/mL sulfamethoxazole, 0.18 mg/mL trimethoprime) by adding 22.75 mL of Bactrim/Septra to each liter of water once per week as prophylaxis. A light/dark cycle of 12 hours each was strictly adhered to, as was a room temperature of 70-75^{o}F. Animals remained within the confines of the Micro-Isolators except for scheduled cage changes and treatments, which were performed in a laminar flow hood. Ibuprofen was used as a pain reliever to reduce the discomfort associated with treatment or inoculation of leukemia cells. In some experiments, NOD/SCID mice (6-8 week old, female, same age in all cohorts in each

independent experiment) were inoculated intravenously (i.v) with ALL xenograft cells (2 x10^6 leukemia cells in 0.2 mL PBS) via tail vein injection with a 27-gauge needle. Mice were then treated on day 1 (2^{nd} passage cells from Xeno Case #7 and Xeno Case #11) with CD19L-sTRAIL (17 fmol/kg/day administered intravenously via tail vein injections on 2 consecutive days) or 2 Gy TBI. Untreated mice challenged with the same number of leukemia cells were included as controls. Mice were monitored daily and electively euthanized by CO_2 asphyxia when any mouse developed morbidity. Blood was collected by cardiac puncture after euthanasia for complete blood counts (CBC) on a Bayer Advia 120 (San Diego, CA) blood analyzer and standard serum chemistry tests using an Olympus AU5400 (Sacramento, CA) instrument. Peripheral smears were stained with Wright-Giemsa and examined microscopically for the presence of circulating leukemia cells. Images were taken with an EVOS XL Core Light Microscope (AMG Bothel, WA) using 20X and 40X objectives. At the time of their elective sacrifice, mice were necropsied to confirm leukemia-associated splenomegaly. Spleens of mice were removed, measured, and cell suspensions were prepared for determination of mononuclear cell counts. Multiple organs were preserved in 10% neutral phosphate buffered formalin, and processed for histologic sectioning. For histopathologic studies, formalin fixed tissues were dehydrated and embedded in paraffin by routine methods. Glass slides with affixed 4-5 micron tissue sections were prepared and stained with Hemotoxylin and Eosin (H&E). Brain, liver, kidney, lymph nodes, and bone marrow were examined for their leukemic involvement. Organs were examined for toxic lesions as in C57BL/6 mice. Images were taken with an EVOS XL Core Light Microscope (AMG Bothel, WA) using 20X and 40X objectives. For the analysis of the *in vitro* potency of various treatments against leukemic stem cells in xenograft specimens, two-tailed T-tests with correction for unequal variance (Microsoft, Excel) were performed comparing the mean spleen size, cellularity as well as absolute lymphocyte counts (ALC) for the various treatments. We also examined the effect of CD19L-sTRAIL on the event-free survival (EFS) outcome of NOD/SCID mice with xenografted advanced BPL: Mice were inoculated i.v. with xenograft cells (2x10^6 cells/mouse) derived from primary leukemia cells of two relapsed

BPL patients (BPL Xenograft Clone #7 and BPL Xenograft Clone #11). In the first model that employed Xenograft Clone #7, 11 CON mice were left untreated. 11 test mice with symptomatic xenografted BPL were treated with CD19L-sTRAIL as a single agent (24 fmol/kg over 2 days with commencement on day 6: N=5; 51 fmol/kg over 3 days with commencement on day 10: N=6). 13 test mice were treated with chemotherapy administered as a cocktail on day 10: 6 mice were treated with Vincristine (0.05 mg/kg) + Doxorubicin (2 mg/kg) + PEG-Asparaginase (850 IU/kg) and 7 mice were treated with Vincristine (0.05 mg/kg) + Dexamethasone (2 mg/kg) + PEG-Asparaginase (850 IU/kg). 5 test mice with symptomatic xenografted BPL were treated with a single dose of 17 fmol/kg CD19L-sTRAIL on day 6. In the second model, intravenous inoculation of NOD/SCID mice with $2x10^6$ of Xenograft Clone #11 cells invariably causes rapidly progressive CNS leukemia with meningeal involvement on day 3 and evidence of diffuse multiorgan involvement on day 6. Of the 19 control mice, 14 were left untreated and 5 received a single dose TBI (2 Gy) on day 2. Fourteen test mice with symptomatic advanced leukemia received a single dose of 34 fmol/kg CD19L-sTRAIL on day 10 and additional 5 asymptomatic test mice received 17 fmol/kg/day CD19L-sTRAIL on days 1 and 2. For the analysis of the NOD/SCID mouse xenograft data on the in vivo potency of CD19L-sTRAIL, event-free survival (EFS) times were measured from the day of inoculation of xenograft cells to the day of death or killing for test mice treated with CD19L-sTRAIL. The probability of survival was determined and the event-free interval curves were generated using the Kaplan-Meier product limit method, as in previous studies (6). Log-rank tests were performed to compare differences in median survival estimates between all groups and pairwise comparison of CON vs. CD19L-sTRAIL and Chemotherapy vs. CD19L-sTRAIL-treated mice. Single dose CD19L-sTRAIL and chemotherapy groups were also compared to CON.

In other experiments aimed at evaluating the effects of CD19L-sTRAIL on the leukemia-initiating cells (i.e. putative leukemic stem cell fractions capable of engrafting and causing overt leukemia in NOD/SCID mice) in the BPL xenograft samples (6), leukemia cells (cell density: $2x10^6$ cells/ml)

isolated from spleens of xenografted mice challenged with primary leukemic cells from 5 pediatric BPL patients (4 newly diagnosed and one relapse patient) (viz.: Xeno Case #'s 1, 2, 3, 10 and 11) were (i) irradiated with 2 Gy γ-rays, (ii) treated for 24 h at 37^{o}C with CD19L-sTRAIL at a concentration of 2.1 pM, 25 nM CD19L, or 250 nM sTRAIL, or (iii) left untreated for 24 h at 37^{o}C and then reinjected (Pretreatment cell number of inoculum samples: 150,000 cells/mouse for Xeno Case #3, 250,000 cells/mouse for Xeno Case #'s 1, 2, and 10 and 400,000 cells/mouse for Xeno Case #11) into NOD/SCID mice. Significant treatment effects were determined using linear contrast models defined by one fixed factor for treatment and one random factor to control for multiple measurements taken from each "case". Two separate models were constructed for spleen size and $\log_{10}$ transformed spleen counts. Linear combination of parameters setting the CON group to "1" or setting the CD19L, sTRAIL and RAD groups each to "0.33" measured the effect size for CD19L-sTRAIL (set to "-1") versus CON or "Other Treatments" respectively. Mice injected with *in vitro* treated xenograft cells were monitored and processed in the same fashion as described above for mice injected with untreated xenograft cells that were subjected to various systemic treatment protocols. For the analysis of the *in vitro* potency of various treatments against leukemic stem cells in xenograft specimens, two-tailed T-tests with correction for unequal variance (Microsoft, Excel) were performed comparing the mean spleen size and cellularity for the various treatments.

References

1. Uckun FM, Sun L, Qazi S, Ma H, Ozer Z. Recombinant human CD19-ligand protein as a potent anti-leukemic agent. Br J Haematol. 2011; 153(1):15-23

2. Stieglmaier J, Bremer E, Kellner C, Liebig TM, ten Cate B, Peipp M, Schulze-Koops H, Pfeiffer M, Bühring HJ, Greil J, Oduncu F, Emmerich B, Fey GH, Helfrich W. Selective induction of apoptosis in leukemic B-lymphoid cells by a CD19-specific TRAIL fusion protein. Cancer Immunol

Immunother. 2008; 57(2):233-46

3. Uckun FM, Muraguchi A, Ledbetter JA, Kishimoto T, O'Brien RT, Roloff JS, Gajl-Peczalska K, Provisor A, Koller B. Biphenotypic leukemic lymphocyte precursors in CD2+CD19+ acute lymphoblastic leukemia and their putative normal counterparts in human fetal hematopoietic tissues. Blood. 1989; 73(4):1000-1015.

4. Uckun FM, Qazi S, Ma H, Tuel-Ahlgren L, Ozer Z. STAT3 is a substrate of SYK tyrosine kinase in B-lineage leukemia/lymphoma cells exposed to oxidative stress. Proc. Natl. Acad. Sci. USA 2010; 107(7): 2902-7.

5. Uckun FM, Goodman P, Ma H, Dibirdik I, Qazi S. CD22 Exon 12 Deletion as a Novel Pathogenic Mechanism of Human B-Precursor Leukemia. Proc. Natl. Acad. Sci. USA 2010; 107:16852-16857

6. Uckun FM, Qazi S, Cely I, Sahin K, Shahidzadeh A, Ozercan I, Yin Q, Gaynon P, Termuhlen A, Cheng J, Yiv S. Nanoscale liposomal formulation of a SYK P-site inhibitor against B-precursor leukemia. Blood. 2013; 121(21):4348-54. doi: 10.1182/blood-2012-11-470633.

7. Uckun FM, Ma H, Zhang J, Ozer Z, Dovat S, Mao C, Ishkhanian R, Goodman P, Qazi S. Serine phosphorylation by SYK is critical for nuclear localization and transcription factor function of Ikaros. Proc Natl Acad Sci U S A 2012; 109(44):18072-7. doi: 10.1073/pnas.1209828109.

8. Uckun FM, Morar S, Qazi S. Vinorelbine-Based Salvage Chemotherapy for Therapy-Refractory Aggressive Leukemias. Brit J Haematol. 2006; 135(4): 500-508.

9. Uckun FM, Zheng Y, Cetkovic-Cvrlje M, Vassilev A, Lisowski E, Waurzyniak B, Chen H, Carpenter R, Chen CL. In vivo pharmacokinetic features, toxicity profile, and chemosensitizing activity of alpha-cyano-betahydroxy-beta- methyl-N-(2,5-dibromophenyl)propenamide (LFM-A13), a novel antileukemic agent targeting Bruton's tyrosine kinase. Clin Cancer Res. 2002; 8(5): 1224-1233.

Supplemental Figures

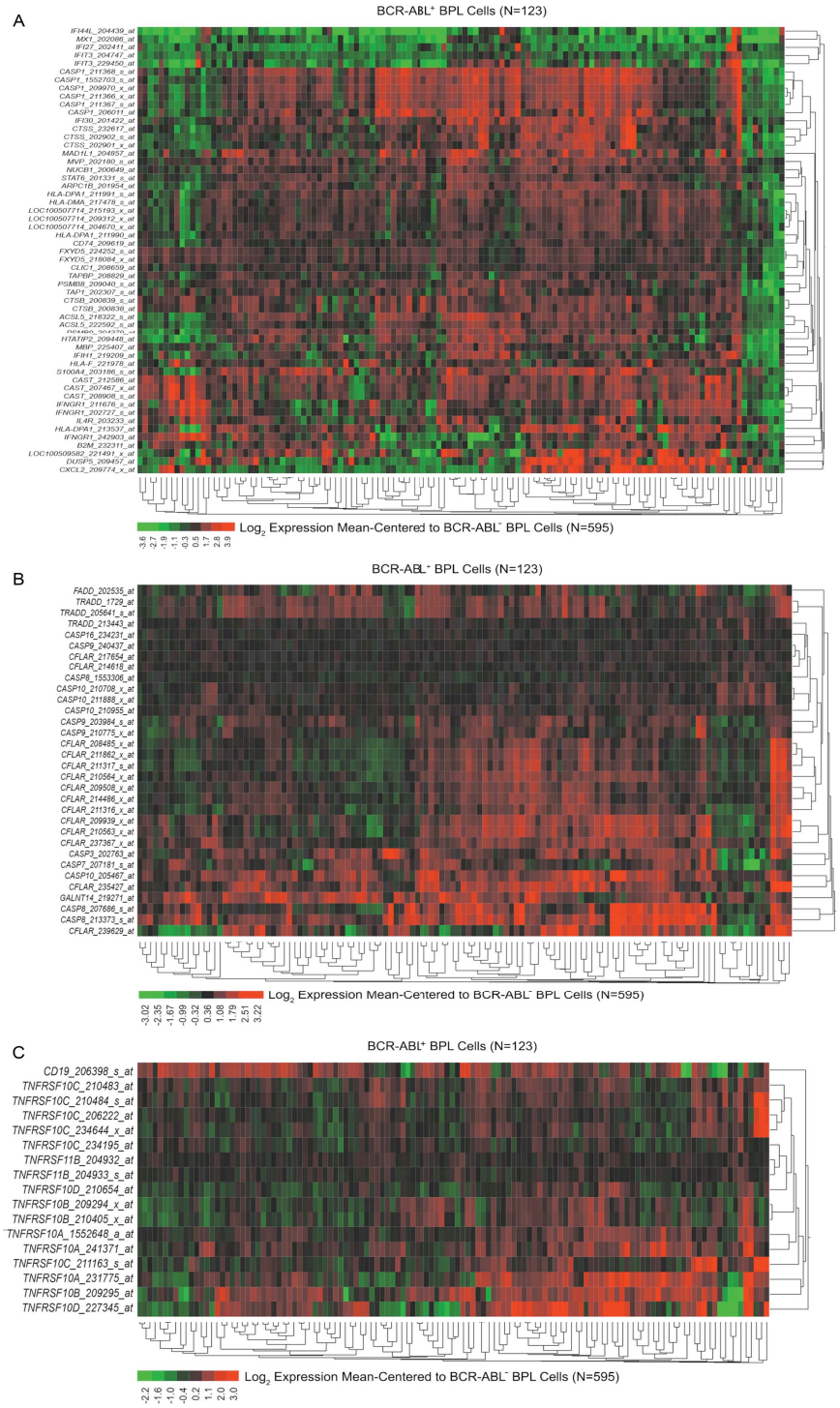

Figure S1. Expression of the molecular signature for TRAIL sensitivity in primary leukemia

cells from BCR-ABL$^+$ BPL patients. Depicted are cluster figures showing the expression levels of those TRAIL sensitivity genes (**Panel A**), regulatory TRAIL pathway genes, including the TRAIL resistance genes CFLAR/CASPER encoding c-FLIP and TRADD as well as TRAIL-sensitivity-associated CASP8 and FADD genes **(Panel B)** and CD19 and TRAIL receptor genes (**Panel C**) that showed highly significant (P-values<0.0001) differential expression between BCR-ABL$^+$ vs. BCR-ABL$^-$ BPL cells. The RMA-normalized gene expression values for leukemia cells obtained from 123 BCR-ABL$^+$ newly diagnosed pediatric BPL patients were log_2-transformed and mean-centered to the average value for leukemia cells from 595 BCR-ABL$^-$ pediatric BPL patients - MLL-R$^+$ and t[1;19]/E2A-PBX1$^+$ patients were excluded. Heat map shows the up and down regulated transcripts for mean-centered expression values and was clustered according to average distance metric.

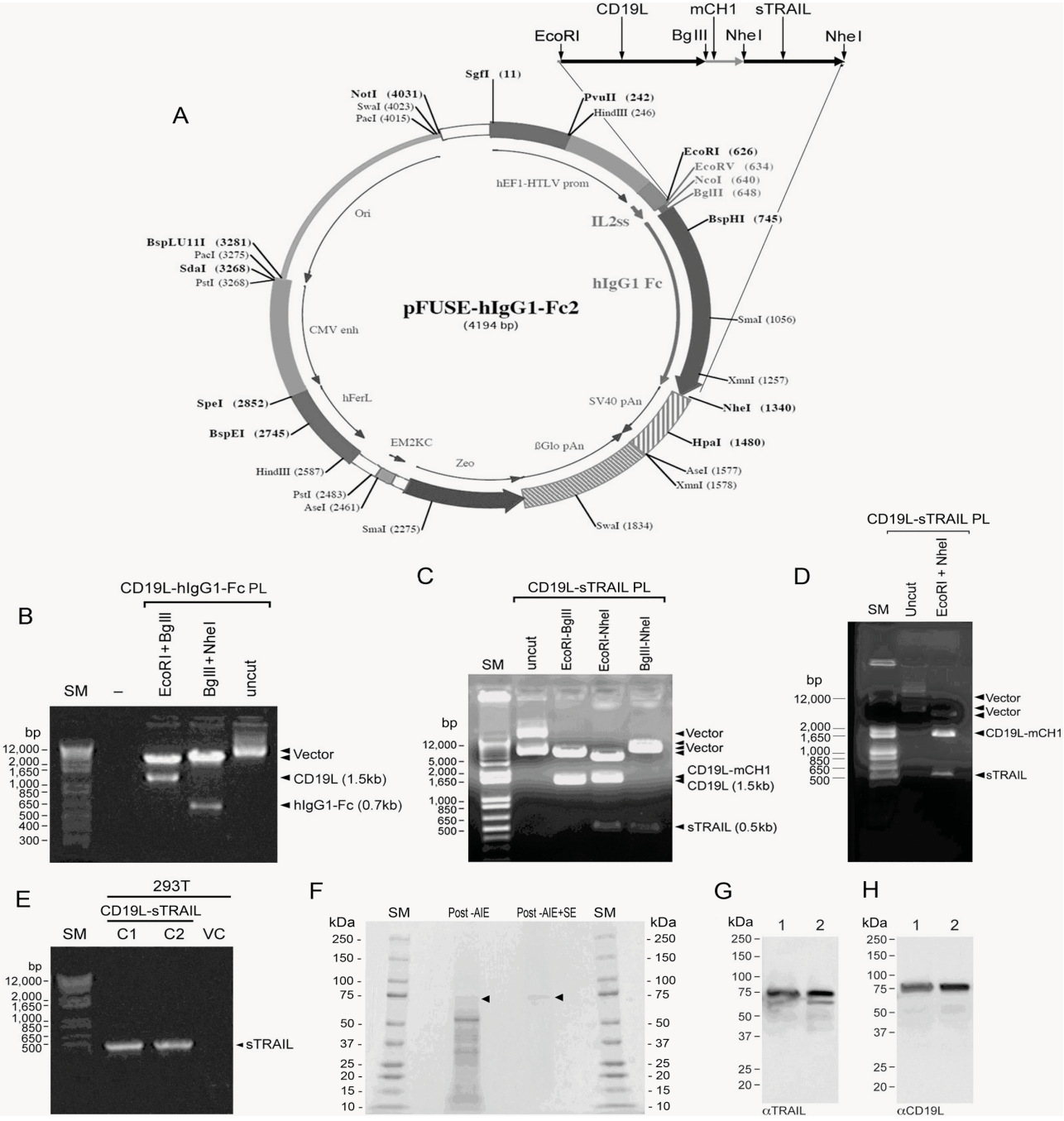

Figure S2. Engineering and expression of recombinant human CD19L-sTRAIL fusion protein. **[A]** Schematic map of the CD19L-sTRAIL expression vector. **[B]** Depicted is a 1% agarose gel confirming the presence of the 1.5-Kb CD19L cDNA and 0.7-Kb hIgG1-Fc

components of this plasmid after restriction enzyme digestion with 20,000U/mL of the respective enzymes. 1 µg of DNA was loaded in each lane. **[C&D]** Restriction enzyme digestion of the pFUSE-CD19L-Linker-sTRAIL construct confirmed the presence of the CD19L (1.5-Kb), CD19L-mCH1 (1.6-Kb) and the sTRAIL (0.5-kb) cDNA fragments when separated on a 1% agarose gel. C1 and C2 depict the results from two independent experiments. **[E]** HEK-293T cells were transfected with the pFUSE-CD19L-sTRAIL expression construct (two different CD19L-sTRAIL plasmid clones C1 and C2), and empty vector (VC). To confirm the expression of the fusion transcript, total RNA was extracted from transfected cells after 24 hrs. One-step RT-PCR was performed using the sTRAIL cloning primer set (F: 5' AGAGAAAGAGGTCCTCAG, R: 5' TTGGGGCCTTTTTAGTTGGCTAA). A 0.5-Kb PCR product was shown only in the CD19L-sTRAIL-transfected cells, but not in the VC-transfected cells. PL: plasmid; SM: size markers – 1-Kb DNA ladder. **[F]** SDS-PAGE of purified CD19L-sTRAIL under nonreducing conditions. Gel scan analysis of the post-AIE+SE CD19L-sTRAIL lane showed a major band migrating at ~74 kDa representing 85% of the protein in the lane and a minor band migrating at ~70 kDa representing 15% of the protein in the lane. **[G&H]** The sTRAIL and CD19L domains of CD19L-sTRAIL were detected by Western blot analysis using anti-TRAIL and anti-CD19L antibodies.

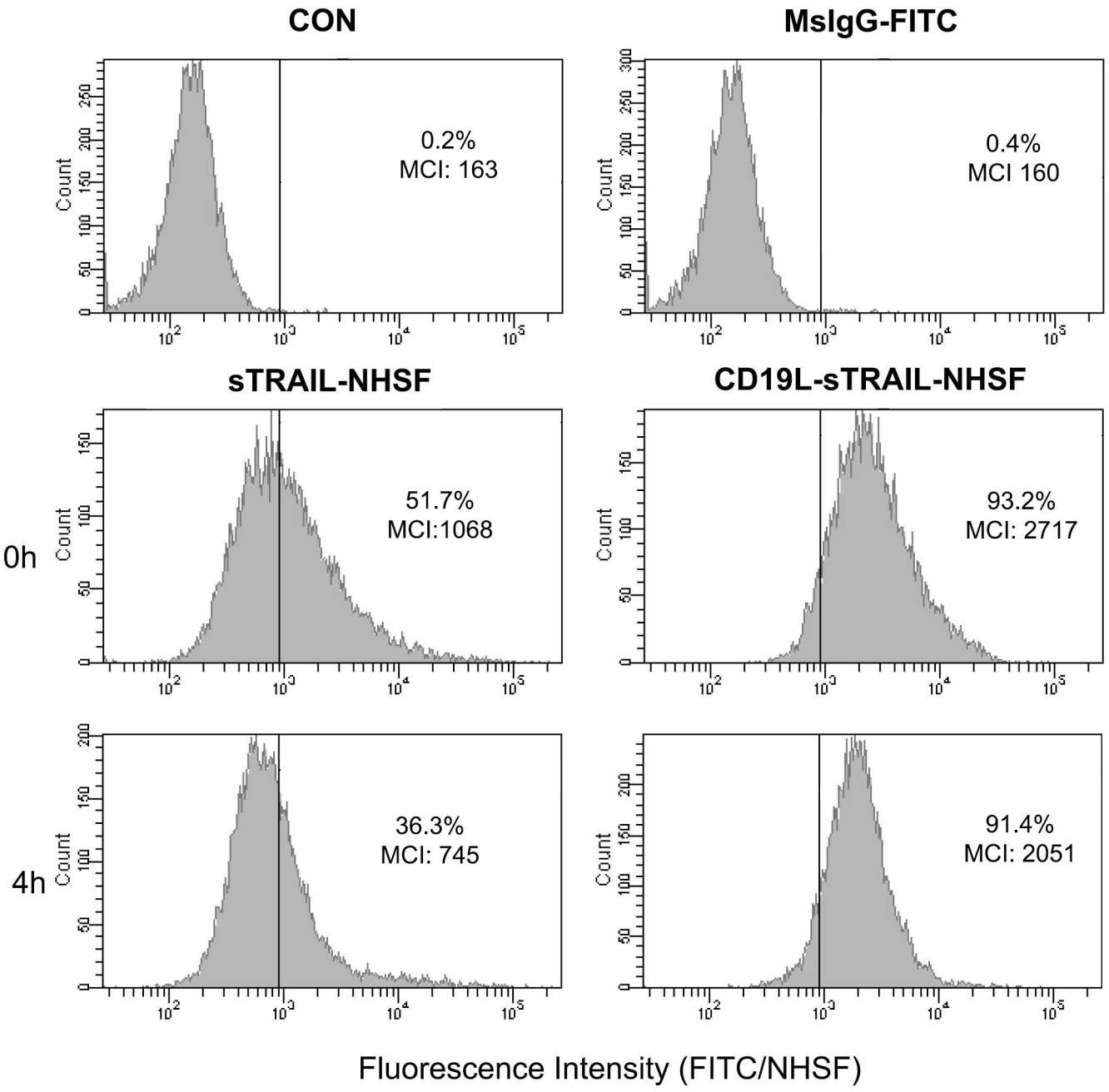

Figure S3. CD19L-sTRAIL binding to human BPL cells is stronger and more stable than sTRAIL binding. Both CD19L-sTRAIL and sTRAIL were fluorescently labeled with NHSF. We compared the binding of CD19L-sTRAIL (20 nM) and sTRAIL (20 nM) to the BCR-ABL^{+} BPL cell line ALL-1 using flow cytometry. Cells were stained for 1 hour on ice, examined either immediately

(0 h) or 4 h after wash with ice-cold PBS for surface associated immunofluorescence using a LSR II flow cytometer. Shown are the values for % positivity compared to the background fluorescence of unstained control samples (CON) as well as control samples stained with a FITC-labeled mouse IgG protein and the mean channel of immunofluorescence (MCI) as a measure of the average surface fluorescence intensity.

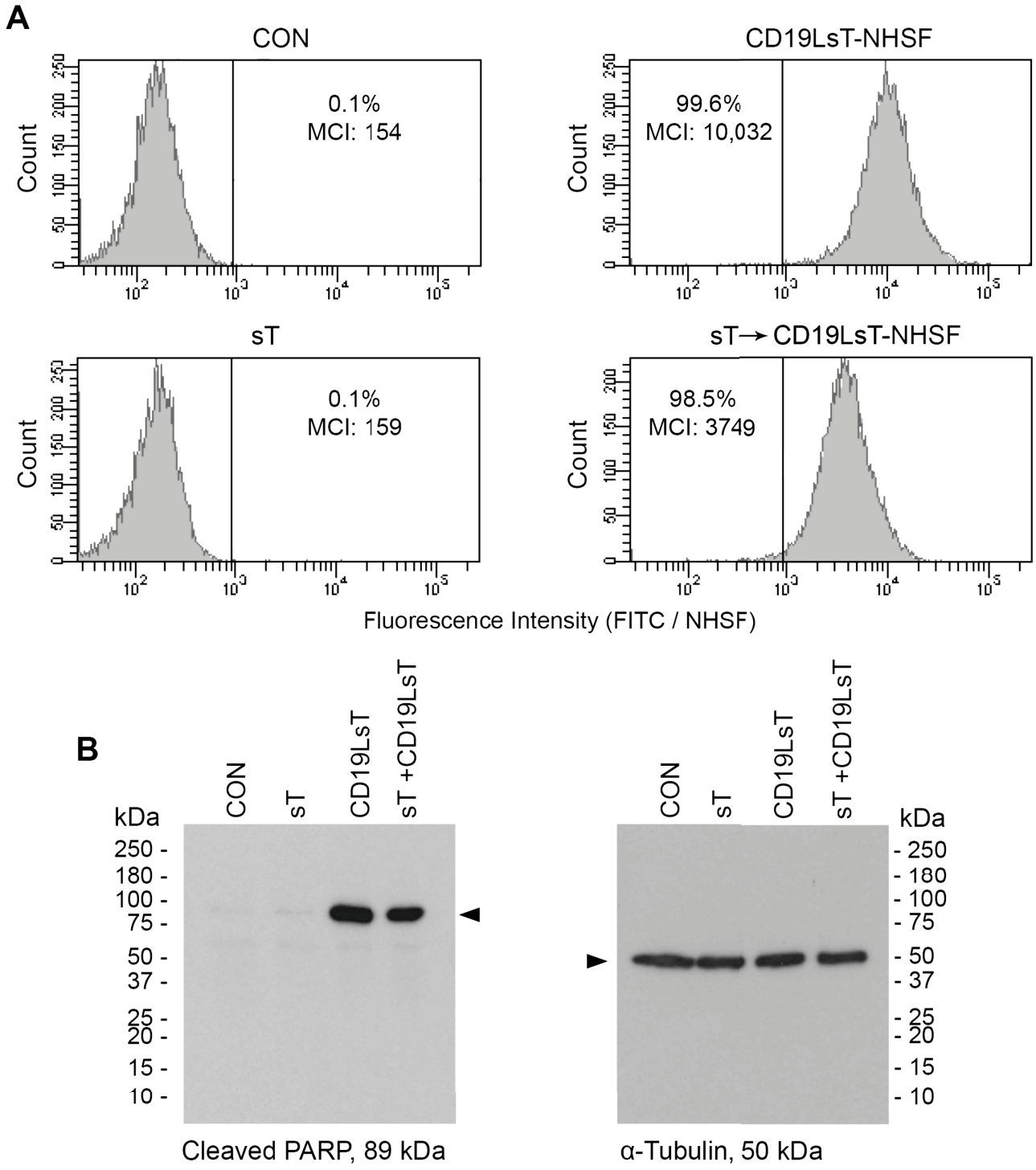

Figure S4. Recombinant sTRAIL does not prevent CD19L-sTRAIL from binding to CD19$^+$ leukemia cells and activating the TRAIL-R linked apoptotic pathway. [A] CD19L-sTRAIL (CD19LsT) was fluorescently labeled with NHSF. We subsequently compared the binding of the NHSF-labeled CD19L-sTRAIL (20 pM) in the presence or absence of a 50-fold molar excess (1

nM) of unlabeled sTRAIL (sT) to the BCR-ABL$^+$ BPL cell line ALL-1 using flow cytometry. Cells were stained for 1 hour on ice and examined immediately after washing with ice-cold PBS, for surface associated immunofluorescence using a LSR II flow cytometer. Shown are the respective FACS histograms along with values for % positivity compared to the background fluorescence of unstained control samples (CON) as well as control samples stained with a FITC-labeled mouse IgG protein and the mean channel of immunofluorescence (MCI) as a measure of the average surface fluorescence intensity. **[B]** Depicted are Western blots documenting the TRAIL-R linked death pathway activation in CD19LsT-treated ALL-1 cells by detection of the 89-kDa cleaved product of PARP without a change in the amount of the 50-kDa tubulin. CD19LsT was used at a 20 pM concentration either alone or in combination with a 50-fold molar excess (1 nM) of sT. Controls included samples treated with 1 nM sT in the absence of CD19LsT.

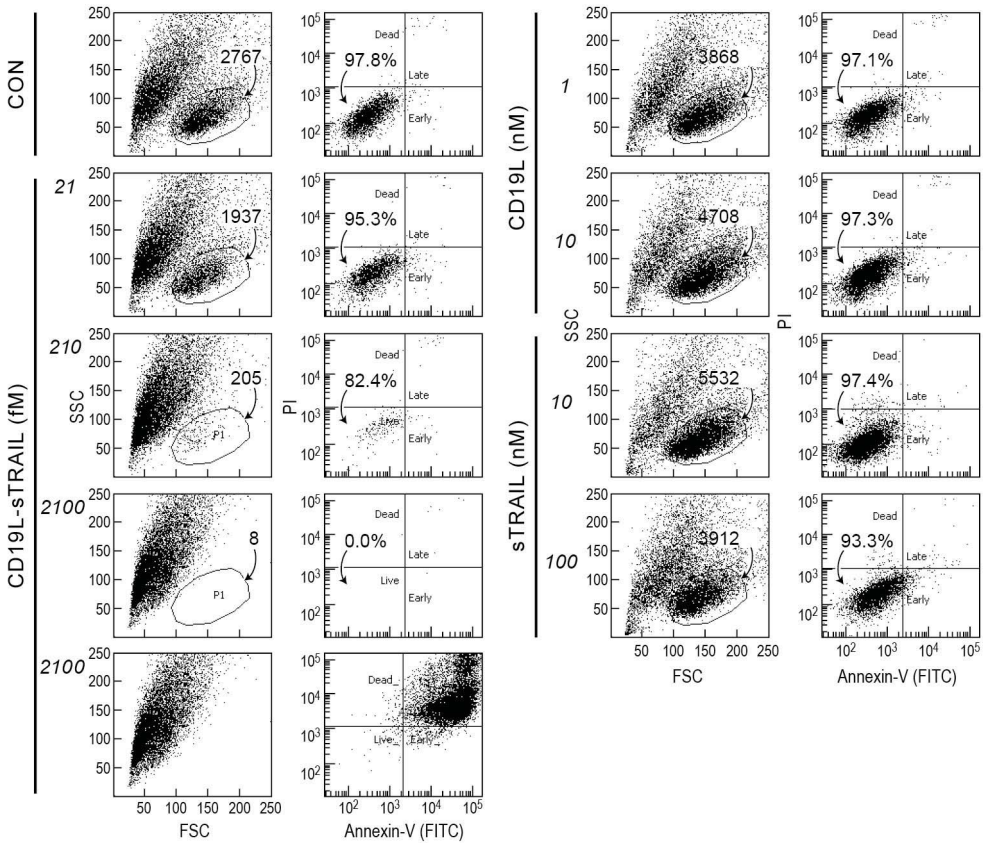

Figure S5. In vitro anti-leukemic potency of CD19L-sTRAIL against CD19$^+$ human BPL cells. ALL-1 cells were treated for 48h at 37^{o}C with 21-2100 fM CD19L-sTRAIL, 1-10 nM CD19L, or 10-100 nM sTRAIL. Controls include untreated cells (CON). Cells were analyzed for apoptosis using the standard quantitative flow cytometric apoptosis assay with the Annexin V-FITC Apoptosis Detection Kit (Sigma, Catalog # APOAF-50TST). The labeled cells were analyzed on a LSR II flow cytometer. The anti-leukemic potency of CD19L-sTRAIL is evidenced by the significantly lower percentages of Annexin V-FITC$^-$PI$^-$ live cells located in the left lower quadrant of the corresponding two-color fluorescence dot plots within the P1 lymphoid window as well as substantially higher percentage of Annexin V-FITC$^+$PI$^+$ apoptotic cells located in the right upper quadrant with marked shrinkage and altered SSC as well as decreasing numbers of remaining cells in the P1 lymphoid

window in the corresponding FSC/SSC light scatter plot from the 10,000 cells analyzed. The lowest panel depicts the Annexin-V-FITC/PI staining of the total cell population, confirming the near complete apoptosis of the total cell population, as evidenced by the Annexin-V-FITC/PI-double positivity. Unlike CD19L-sTRAIL that caused apoptosis with <10% of the target leukemia cells remaining alive after treatment with 210 fM (([205x0.824/2767x0.978] x100 = 6.2%) or 2.1 pM (8x0/2767x0.978 = 0%) CD19L-sTRAIL, neither CD19L nor sTRAIL caused apoptosis of ALL-1 cells even at the >3-log higher nanomolar concentrations applied.

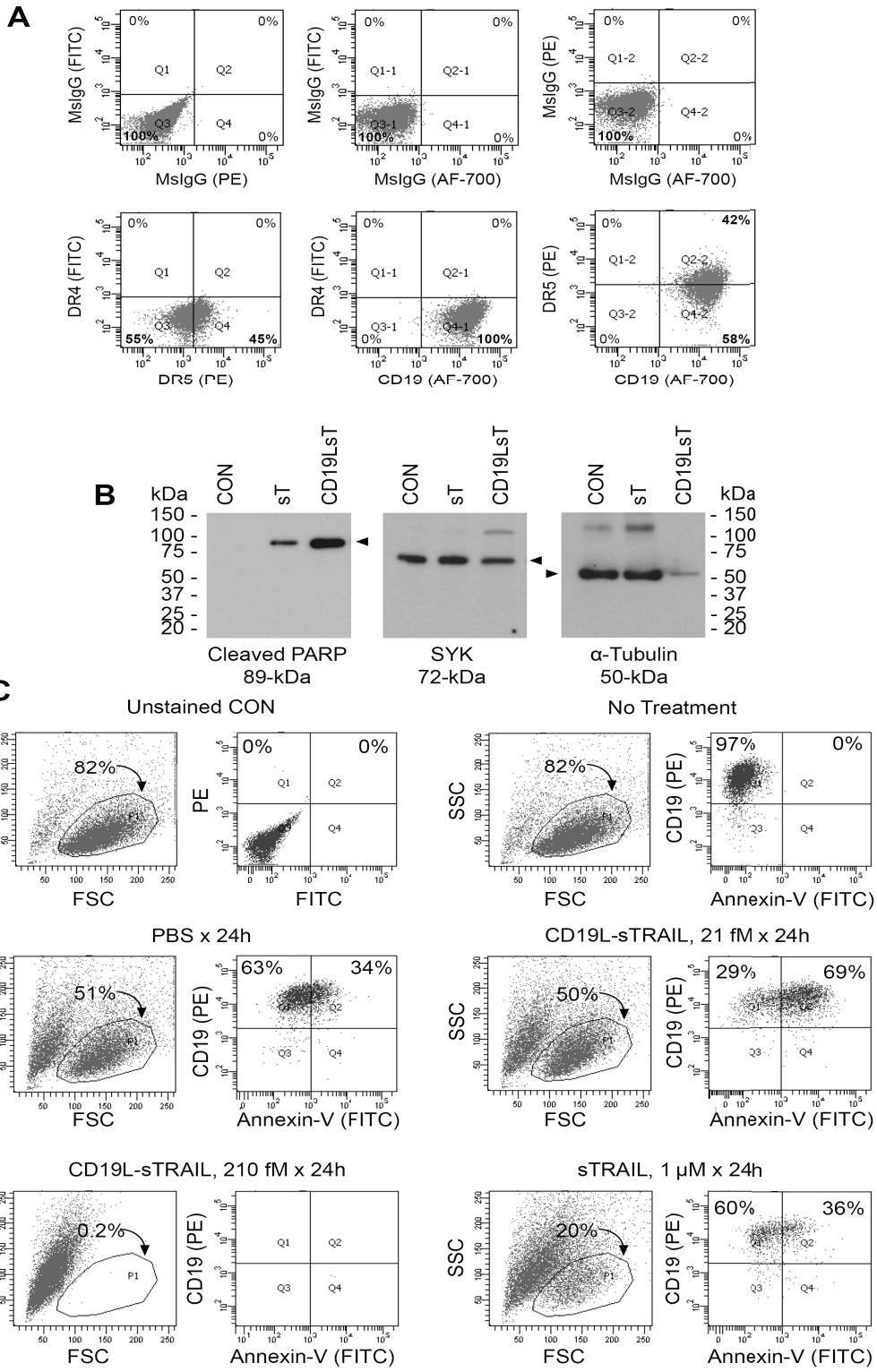

Figure S6. CD19L-sTRAIL (CD19LsT) delivers a stronger apoptotic signal than sTRAIL (sT).

[A] A sT-sensitive subclone of the ALL-1 cell line (designated ALL-1$^{sT\text{-}S}$) was stained by direct

immunofluorescence for CD19, DR4, and DR5. Controls included cells stained with isotype-matched mouse IgG. Depicted are the FACS-correlated two-color fluorescence dot plots. **[B]** Depicted are Western blots documenting the TRAIL-R linked death pathway activation in CD19LsT (20 pM)-treated vs. sT (1 nM)-treated ALL-1^{sT-S} cells by detection of the 89-kDa cleaved product of PARP. Controls included Western blots using anti-SYK and anti-α-Tubulin antibodies. **[C**] ALL-1^{sT-S} cells were treated for 24h at 37^{o}C with 21 or 210 fM CD19L-sTRAIL vs. 1 µM sT. Controls included untreated cells (CON) as well as cells treated with PBS x 24h. Cells were analyzed for apoptosis using a quantitative flow cytometric apoptosis assay in which they were stained with a PE-labeled anti-CD19 MoAb plus Annexin V-FITC (8). The labeled cells were analyzed on a LSR II flow cytometer. The anti-leukemic potency of 21 fM CD19L-sTRAIL is evidenced by the significantly lower percentages of Annexin V-$FITC^{-}CD19^{+}$ live ALL-1^{sT-S} cells located in the left lower quadrant of the corresponding two-color fluorescence dot plots within the P1 lymphoid window as well as substantially higher percentage of Annexin V-$FITC^{+}PI^{+}$ apoptotic cells located in the right upper quadrant with marked shrinkage and altered SSC as well as decreasing numbers of remaining cells in the P1 lymphoid window in the corresponding FSC/SSC light scatter plot from the 10,000 cells analyzed.

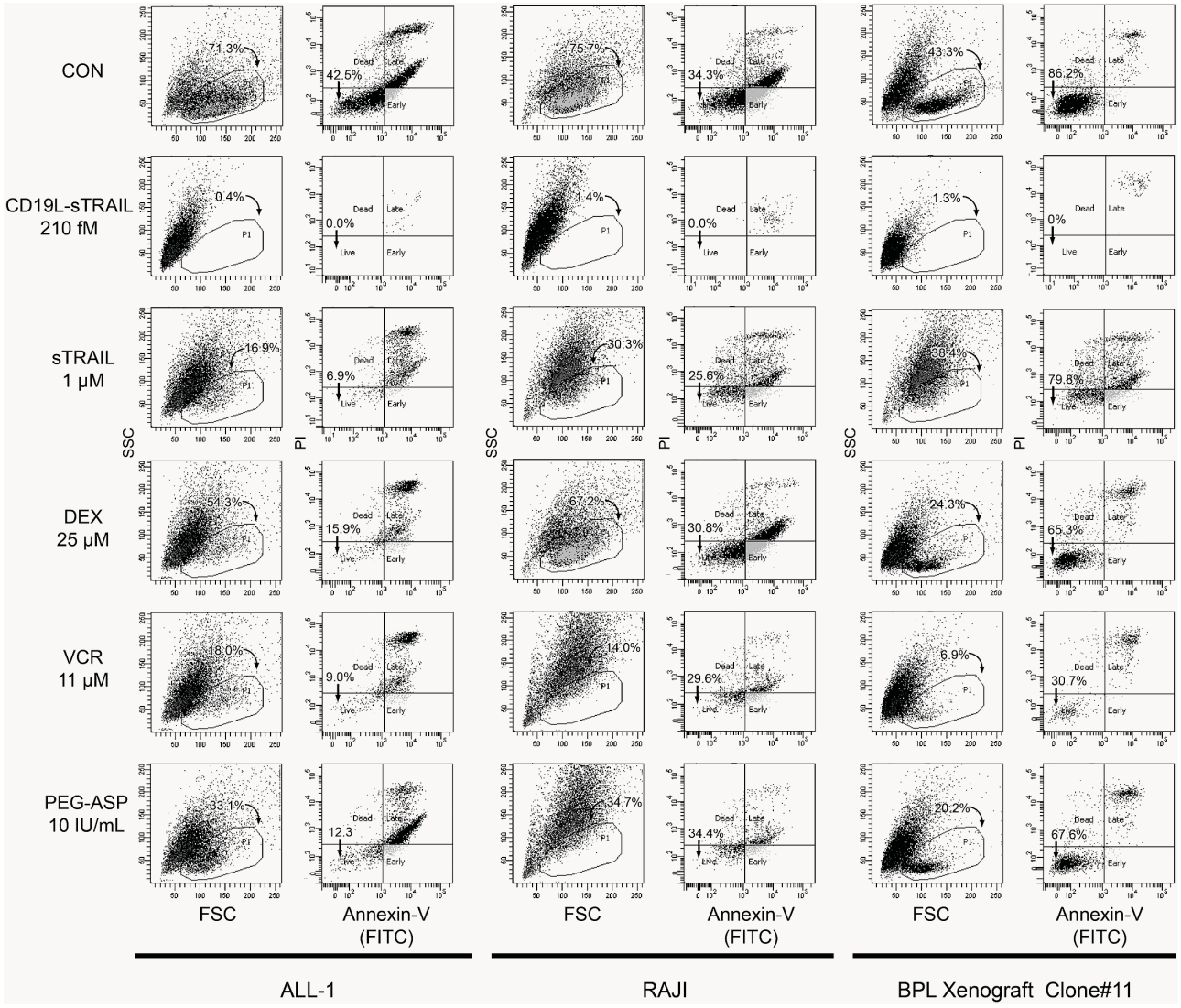

Figure S7. In vitro anti-leukemic potency of CD19L-sTRAIL, sTRAIL, and standard chemotherapeutic drugs. Cells were treated for 48h at 37^{o}C with 210 fM CD19L-sTRAIL vs. 1 µM sT or standard chemotherapy drugs at the indicated concentrations. Controls included sham-treated cells (CON) cultured x 48h. Cells were analyzed for apoptosis using the standard quantitative flow cytometric apoptosis assay with the Annexin V-FITC Apoptosis Detection Kit (Sigma, Catalog # APOAF-50TST). The labeled cells were analyzed on a LSR II flow cytometer. The superior anti-leukemic potency of CD19L-sTRAIL is evidenced by the significantly lower percentages of Annexin V-FITC^{-}PI^{-} live cells located in the left lower quadrant of the corresponding two-color fluorescence dot plots within the P1 lymphoid window as well as a marked shrinkage and

altered SSC as well as decreasing numbers of remaining cells in the P1 lymphoid window in the corresponding FSC/SSC light scatter plot from the 10,000 cells analyzed.

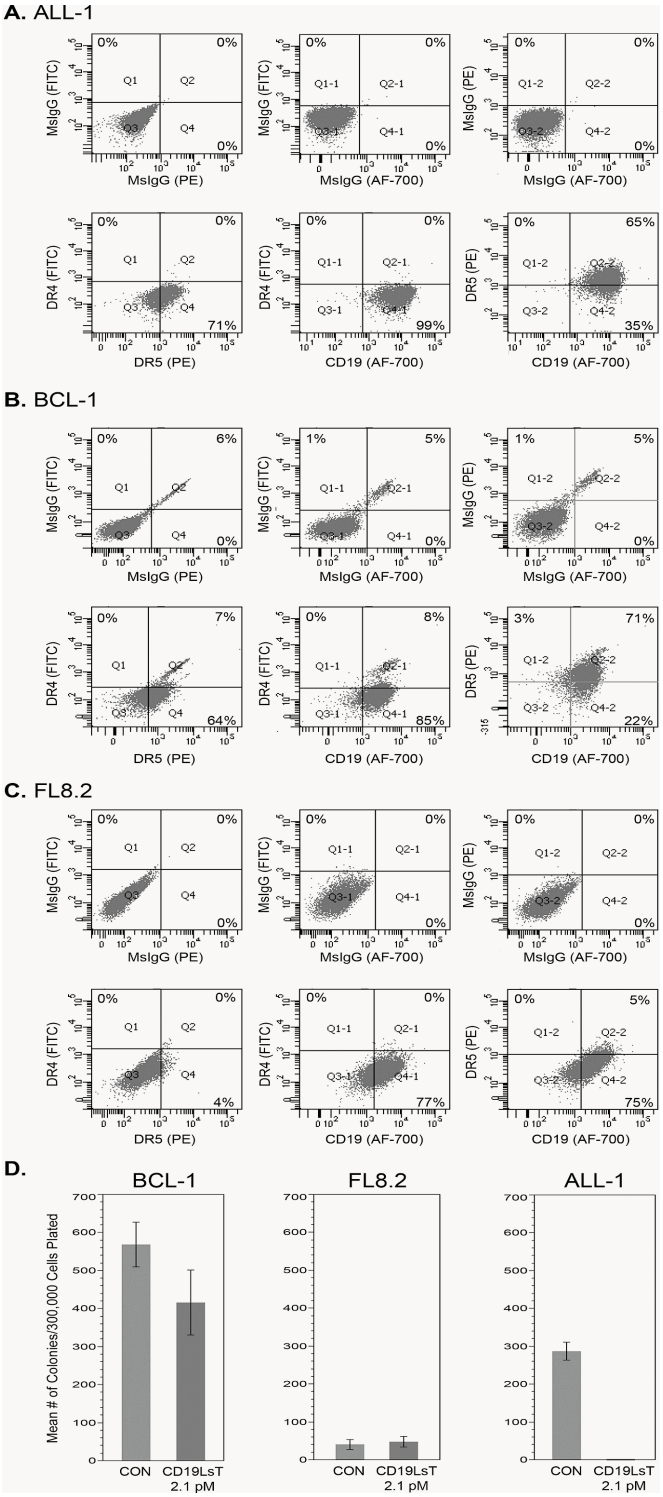

Figure S8. Sensitivity of non-leukemic human pro-B and B-cells to CD19L-sTRAIL.[A-C]

Cells were stained by direct immunofluorescence for CD19, DR4, and DR5. Controls included cells stained with isotype-matched mouse IgG. Depicted are the FACS-correlated two-color

fluorescence dot plots. **[D]** Depicted are the bar graphs showing the mean number of colonies per 300,000 cells plated for the BPL cell line ALL-1, the fetal liver derived pro-B cell line FL8.2 and the mature B-cell line BCL-1.

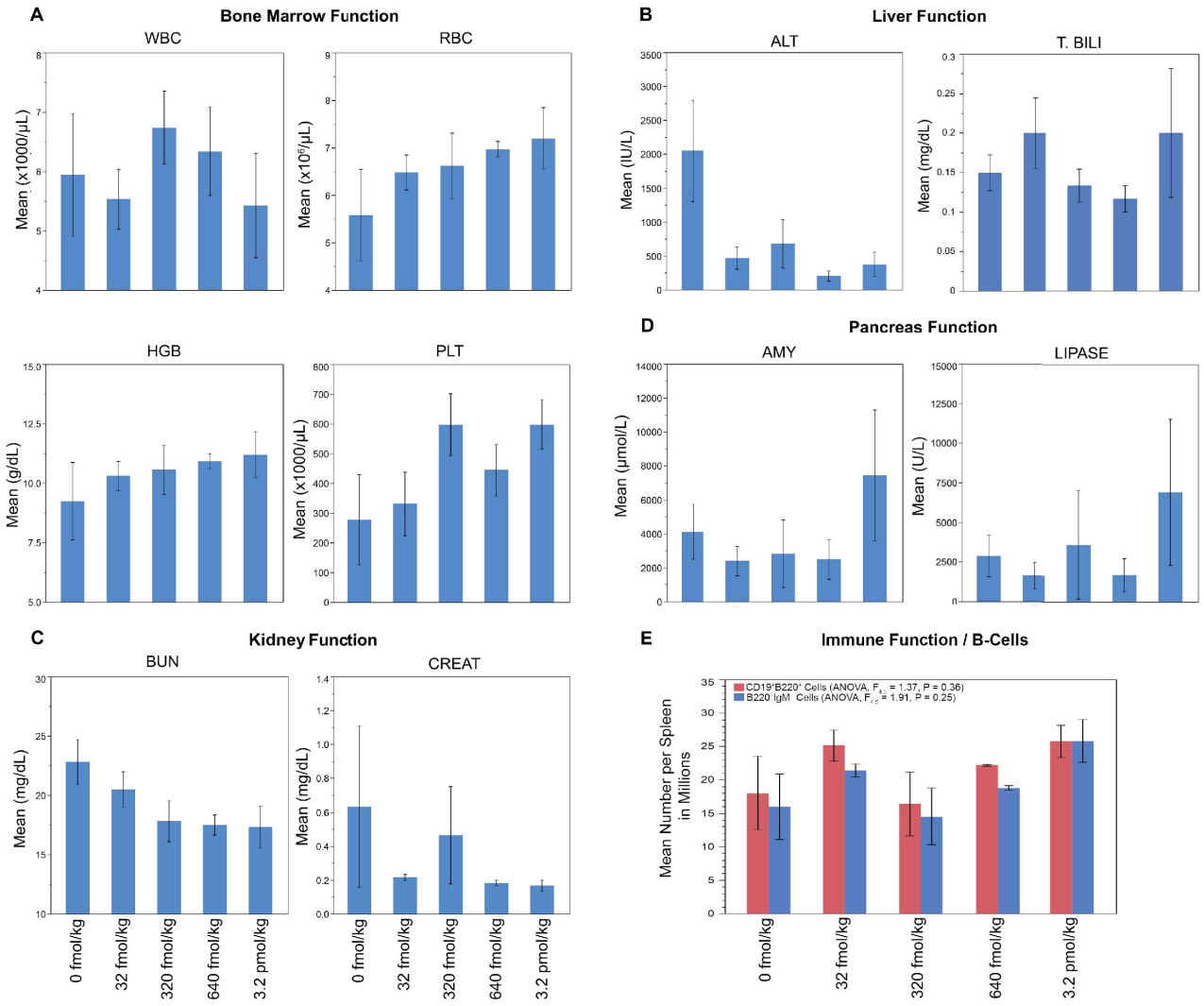

Figure S9. Toxicity profile of CD19L-sTRAIL in C57BL/6 mice. [A-D] Groups of 6 mice were treated with intravenous single dose bolus tail vein injections of CD19L-sTRAIL at one of the 4 different dose levels, ranging from 32 fmol/kg to 3.2 pmol/kg. Mice were monitored daily for signs of morbidity and electively sacrificed on day 28 to determine the toxicity of CD19L-sTRAIL by examining their blood chemistry profiles, blood counts, and evaluating multiple organs for the presence of toxic lesions. Depicted are the bar graphs showing the mean values for each organ function parameter determined. No statistically significant changes were observed that suggested a CD19L-sTRAIL related adverse effect on the function of bone marrow, liver, kidney, or pancreas. There were no toxic lesions suggestive of any significant parenchymal organ damage

(**supplemental Table 2**). **[E]** Depicted are the bar graphs showing mean number of $B220^{+}CD19^{+}$ and $B220^{+}sIgM^{+}$ B-lineage lymphoid cells per spleen for each of the 5 groups of mice evaluated in the C57BL/6 toxicity study.

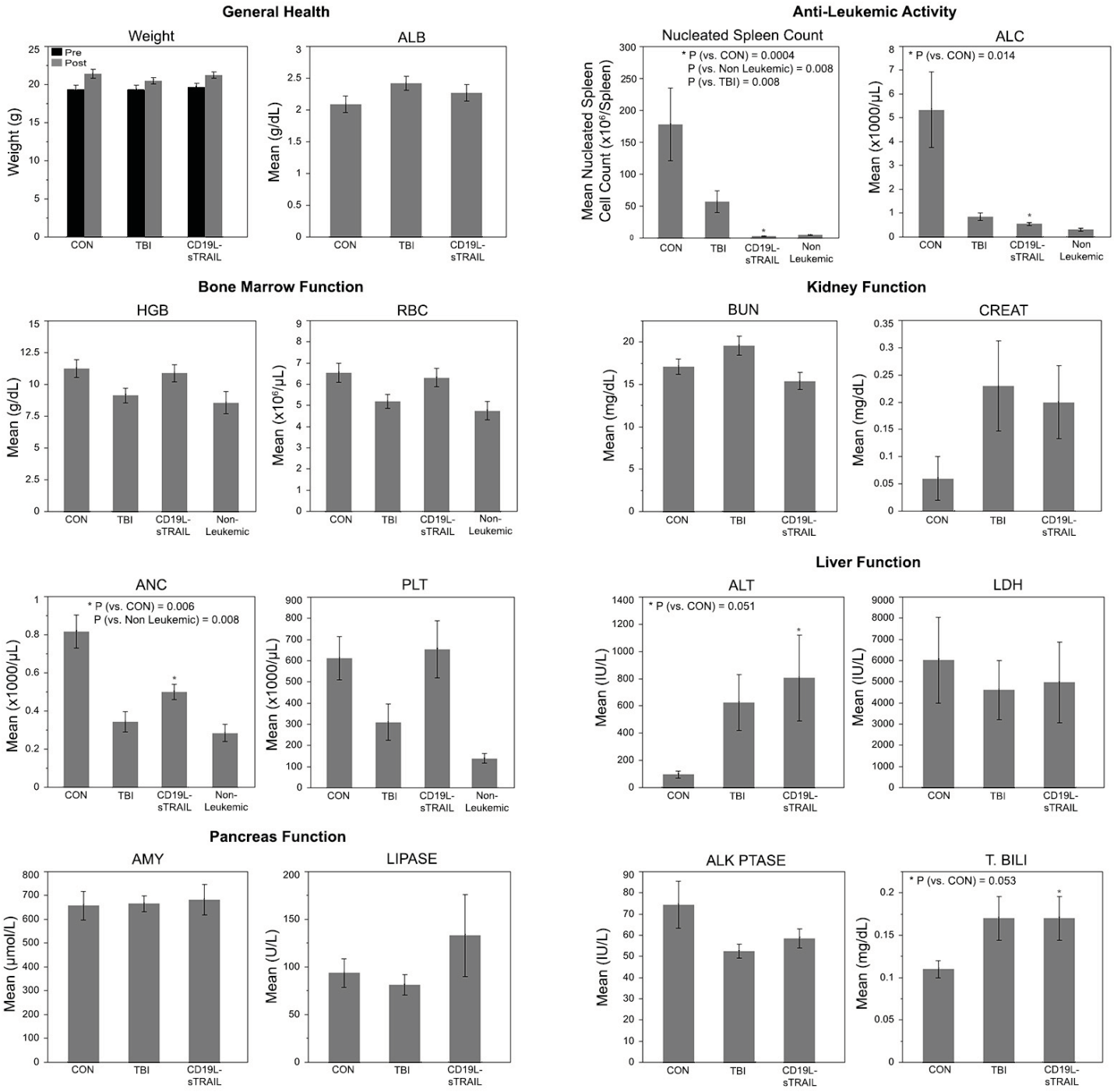

Figure S10. In vivo anti-leukemic activity and toxicity of CD19L-sTRAIL in NOD/SCID mouse models of relapsed BPL. NOD/SCID mice (5/group/xenograft model x 2 models; 10 mice/treatment group cumulatively) were inoculated with $2x10^6$ xenograft cells derived from 2 relapsed BPL patients. CD19L-sTRAIL was administered intravenously for 2 days (days 1 and 2)

at a non-toxic daily dose level of 17 fmol/kg/day. One of the treatment groups received TBI (2 Gy, day 2). The experiment was terminated by euthanasia of all mice in all treatment groups when untreated control mice (CON) showed signs of morbidity on day 19. Depicted are the bar graphs showing the mean values for each organ function parameter determined as well as nucleated spleen cell count and absolute lymphocyte count (ALC) as measures of the leukemia burden. While control mice and TBI-treated mice had splenomegaly with high nucleated spleen cell counts and elevated ALC values due to circulating leukemia cells, mice treated with CD19L-sTRAIL had normal spleen size, normal nucleated spleen cell counts and ALC values that were similar to those of non-leukemic control NOD/SCID mice which were not inoculated with any leukemia cells.

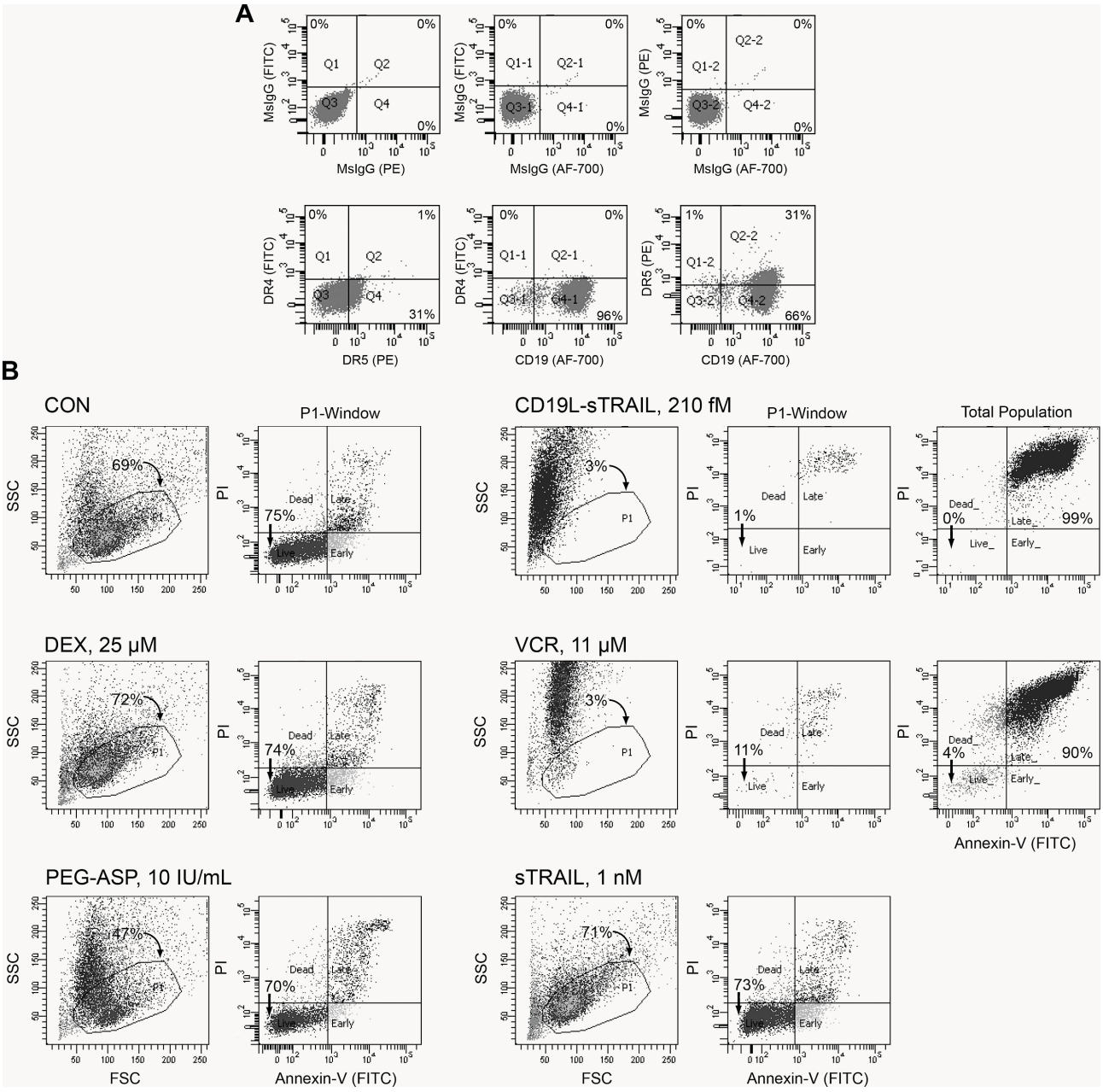

Figure S11. Immunophenotype and Drug Sensitivity of BPL Xenograft Clone #7 Used in NOD/SCID Mouse EFS Experiments. **[A]** Cells were stained by direct immunofluorescence for CD19, DR4, and DR5. Controls included cells stained with isotype matched mouse IgG. Depicted are the FACS-correlated two-color fluorescence dot plots. **[B]** Cells were treated for 24h at 37^{o}C with 210 fM CD19L-sTRAIL vs. 1 nM sT or standard chemotherapy drugs at the indicated concentrations. Controls included sham-treated cells (CON) cultured x 24h. Cells were analyzed

for apoptosis using the standard quantitative flow cytometric apoptosis assay with the Annexin V-FITC Apoptosis Detection Kit (Sigma, Catalog # APOAF-50TST). The labeled cells were analyzed on a LSR II flow cytometer. The superior anti-leukemic potency of CD19L-sTRAIL is evidenced by the significantly lower percentages of Annexin V-FITC$^-$PI$^-$ live cells located in the left lower quadrant of the corresponding two-color fluorescence dot plots within the P1 lymphoid window as well as a marked shrinkage and altered SSC as well as decreasing numbers of remaining cells in the P1 lymphoid window in the corresponding FSC/SSC light scatter plot from the 10,000 cells analyzed.

Table S1. Expression of TRAIL-sensitivity determining gene cassettes in primary BPL cells

	BCR-ABL^{+} / Others^{A}	
	Mean Fold Difference	**Linear Contrast P-value**
TRAIL sensitivity (146 probesets, 68 genes)	1.21	1.0E-10
IFI44L_204439_at	0.38	9.5E-49
CASP1_211368_s_at	2.39	4.6E-40
CAST_212586_at	2.09	2.5E-29
TRAIL Receptors (17 probesets, 7 genes)	1.15	1.0E-10
TNFRSF10B_209295_at	1.56	6.3E-21
CD19_206398_s_at	1.46	1.5E-15
TNFRSF10A_231775_at	1.42	6.2E-14
TRAIL pathway (32 probesets, 10 genes)	1.28	5.0E-26
CASP8_213373_s_at	2.33	5.6E-69
CASP10_205467_at	1.99	2.0E-46
GALNT14_219271_at	1.94	1.6E-43
	E2A-PBX1^{+}/ Others^{A}	
	Mean Fold Difference	**Linear Contrast P-value**
TRAIL sensitivity (146 probesets, 68 genes)	0.84	1.2E-05
IFI44_214453_s_at	0.20	1.8E-71
IFI44L_204439_at	0.23	2.9E-62
MX1_202086_at	0.41	4.2E-24
TRAIL Receptors (17 probesets, 7 genes)	0.84	1.5E-09
TNFRSF10B_209295_at	0.40	6.7E-46
TNFRSF10D_227345_at	0.52	7.7E-24
CD19_206398_s_at	1.79	1.3E-19
TRAIL pathway (32 probesets, 10 genes)	0.94	3.9E-02
GALNT14_219271_at	3.01	5.2E-64
CASP8_213373_s_at	0.61	3.3E-14
CFLAR_237367_x_at	0.81	1.6E-03
	MLL-R^{+}/ Others^{A}	
	Mean Fold Difference	**Linear Contrast P-value**
TRAIL sensitivity (146 probesets, 68 genes)	1.00	9.0E-01
S100A4_203186_s_at	3.17	9.7E-56
HTATIP2_209448_at	2.50	7.6E-36
IFI44L_204439_at	0.47	1.5E-25
DBI_209389_x_at	2.13	5.2E-25
MX1_202086_at	0.48	3.9E-23
TRAIL Receptors (17 probesets, 7 genes)	0.83	3.0E-14
TNFRSF10D_227345_at	0.41	1.5E-62

TNFRSF10B_209295_at	0.50	4.1E-40
TNFRSF10A_231775_at	0.57	5.3E-26
TRAIL pathway (32 probesets, 10 genes)	1.06	2.9E-02
CASP8_213373_s_at	0.59	1.2E-23
CASP9_203984_s_at	1.53	1.8E-15
FADD_202535_at	1.51	1.6E-14

	Relapsed/Diagnosis[B]	
	Mean Fold Difference	**Linear Contrast P-value**
TRAIL sensitivity (146 probesets, 68 genes)	1.00	9.3E-01
CYP1B1_202437_s_at	2.39	2.0E-15
IFIH1_1555464_at	0.58	7.8E-07
LDLR_202068_s_at	0.65	7.5E-05
TRAIL Receptors (17 probesets, 7 genes)	1.00	9.8E-01
TNFRSF10C_211163_s_at	1.34	1.8E-03
TNFRSF10A_241371_at	0.80	1.7E-02
TNFRSF10C_206222_at	1.09	3.6E-01
TRAIL pathway (32 probesets, 10 genes)	0.96	1.0E-01
CFLAR_235427_at	0.81	2.7E-03
CASP7_207181_s_at	0.87	5.3E-02
CASP8_207686_s_at	0.88	5.5E-02

[A]Differential expression of potential genetic biomarkers for therapeutic TRAIL sensitivity in primary leukemia cells from high-risk BPL patients was determined utilizing publicly available archived gene expression profiles of primary leukemia cells from BCR-ABL$^+$ BPL patients (123 samples from GSE13159 and GSE13351), E2A-PBX1$^+$ BPL patients (61 samples from GSE11877, GSE13159 and GSE13351), patients with multi-lineage leukemia (MLL) gene rearrangements (MLL-R$^+$) (95 samples from GSE11877, GSE13159 and GSE13351) in side by side comparison with gene expression profiles of primary leukemia cells that were negative for each of these high-risk molecular markers (N=595 from GSE11877, GSE13159 and GSE13351).

[B]In addition, an archived dataset on gene expression profiles of primary leukemia cells in matched-pair bone marrow specimens obtained at initial diagnosis and 1st relapse from 49 pediatric patients with BPL (GSE28460) was also interrogated. Probesets representing the TRAIL sensitivity signature, TRAIL-receptor genes including CD19 receptor, and TRAIL receptor-linked death pathway genes were analyzed using mixed models of ANOVA to identify significant differences in

expression transcripts encoded by these genes at both the probeset level and changes in expression of the whole cassette. Effect sizes from differences between least square mean and standard error estimates were used to construct planned linear contrasts to assess the significance of the observed changes in gene expression profiles. Fold difference values and linear contrast P-values are reported for each of the 3 gene cassettes and the most significant differentially expressed probesets for each of the gene cassettes

Table S2. Histopathological Findings in Tissues of C57 BL/6 Mice Treated with Intravenous Bolus Injections of CD19L-sTRAIL

	PBS	CD19L-sTRAIL in 100 µL PBS			
Tissue/Diagnosis/Modifiers	100 µL	32 fmol/kg	320 fmol/kg	640 fmol/kg	3.2 pmol/kg
Bone					
No lesions	3/3 [100%]	6/6 [100%]	6/6 [100%]	6/6 [100%]	6/6 [100%]
Bone Marrow					
No lesions	3/3 [100%]	6/6 [100%]	6/6 [100%]	6/6 [100%]	6/6 [100%]
Brain					
No lesions	3/3 [100%]	6/6 [100%]	6/6 [100%]	6/6 [100%]	6/6 [100%]
Gut					
A. Large Intestine					
No lesions	3/3 [100%]	6/6 [100%]	5/6 [83%]	5/6 [83%]	6/6 [100%]
Incidental finding: MALT*	0/3 [0%]	0/6 [0%]	1/6 [17%]	1/6 [17%]	0/6 [0%]
B. Small intestine					
No significant lesions	3/3 [100%]	6/6 [100%]	5/6 [83%]	6/6 [100%]	6/6 [100%]
Incidental finding: MALT*	0/3 [0%]	0/6 [0%]	1/6 [17%]	0/6 [0%]	0/6 [0%]
Heart					
No lesions	3/3 [100%]	6/6 [100%]	6/6 [100%]	5/6 [83%]	6/6 [100%]
Incidental finding: Mineralization, single focus	0/3 [0%]	0/6 [0%]	0/6 [0%]	1/6 [17%]	0/6 [0%]
Kidney					
No lesions	3/3 [100%]	6/6 [100%]	6/6 [100%]	6/6 [100%]	6/6 [100%]
Liver					
No lesions	0/3 [0%]	0/6 [0%]	1/6 [17%]	0/6 [0%]	0/6 [0%]
Incidental finding 1: Necrosis, mild multifocal, lymphocytic and neutrophilic	3/3 [100%]	6/6 [100%]	5/6 [83%]	6/6 [100%]	4/6 [66%]
Incidental finding 2: Perivenular mild lymphocytic infiltrate, few foci	1/3 [33%]	6/6 [100%]	4/6 [66%]	4/6 [66%]	5/6 [83%]
Lungs					
No lesions	3/3 [100%]	5/6 [83%]	4/6 [66%]	5/6 [83%]	5/6 [83%]
Incidental finding 1: Pleural fibrin, few foci	0/3 [0%]	1/6 [17%]	0/6 [0%]	1/6 [17%]	1/6 [17%]
Incidental finding 2: Fibrin in small cavity in lobe, with mild hemorrhage	0/3 [0%]	0/6 [0%]	1/6 [17%]	0/6 [0%]	0/6 [0%]
Lymph Node					

No lesions	3/3 [100%]	6/6 [100%]	6/6 [100%]	6/6 [100%]	6/6 [100%]
Ovary					
No lesions	3/3 [100%]	6/6 [100%]	6/6 [100%]	6/6 [100%]	6/6 [100%]
Pancreas					
No lesions	2/3 [66%]	6/6 [100%]	6/6 [100%]	4/6 [66%]	5/6 [83%]
Incidental finding 1: Necrosis, mild, single focus	1/3 [33%]	0/6 [0%]	0/6 [0%]	1/6 [17%]	1/6 [17%]
Incidental finding 2: Focal lymphocytic infiltrate	0/3 [0%]	0/6 [0%]	0/6 [0%]	1/6 [17%]	0/6 [0%]
Sciatic Nerve					
No lesions	3/3 [100%]	6/6 [100%]	6/6 [100%]	6/6 [100%]	6/6 [100%]
Skeletal Muscle					
No lesions	3/3 [100%]	6/6 [100%]	6/6 [100%]	6/6 [100%]	6/6 [100%]
Spinal Cord					
No lesions	3/3 [100%]	6/6 [100%]	6/6 [100%]	6/6 [100%]	6/6 [100%]
Thymus					
No lesions	3/3 [100%]	6/6 [100%]	6/6 [100%]	6/6 [100%]	6/6 [100%]
Thyroid					
No lesions	2/3 [66%]	6/6 [100%]	6/6 [100%]	6/6 [100%]	5/6 [83%]
Thyroid absent from tissue	1/3 [33%]	0/6 [0%]	0/6 [0%]	0/6 [0%]	0/6 [0%]
Incidental finding: Mild focal lymphocytic infiltrate	0/3 [0%]	0/6 [0%]	0/6 [0%]	0/6 [0%]	1/6 [17%]
Urinary Bladder					
No lesions	2/3 [66%]	5/6 [83%]	6/6 [100%]	5/6 [83%]	6/6 [100%]
Not present on slide	1/3 [33%]	0/6 [0%]	0/6 [0%]	0/6 [0%]	0/6 [0%]
Incidental finding: Scattered apoptosis in transitional epithelium	0/3 [0%]	1/6 [17%]	0/6 [0%]	1/6 [17%]	0/6 [0%]
Uterus					
No lesions	2/3 [66%]	4/6 [66%]	4/6 [66%]	5/6 [83%]	2/6 [33%]
Incidental finding: Moderate neutrophilic infiltrate at junction with supporting ligament	1/3 [33%]	2/6 [33%]	2/6 [33%]	0/6 [0%]	4/6 [66%]

Table S3. Histopathological Findings in Tissues of BPL-Xenografted NOD/SCID Mice Treated with CD19L-sTRAIL

	Treatment Group		
Tissue/Diagnosis/Modifiers	Control No Treatment	Total Body Irradiation	CD19L-sTRAIL
Bone			
No lesions	5 [100%]	5 [100%]	5 [100%]
Bone Marrow			
Leukemia cells predominate	5 [100%]	0 [0%]	0 [0%]
Megakaryocytes and myeloid precursors present	0 [0%]	5 [100%]	5 [100%]
Brain			
No parenchymal lesions	5 [100%]	5 [100%]	5 [100%]
Meninges, leukemia cells present	5 [100%]	0 [0%]	0 [0%]
Gut			
A. Large Intestine No lesions	5 [100%]	5 [100%]	5 [100%]
B. Small intestine No lesions	5 [100%]	5 [100%]	5 [100%]
Heart No lesions	5 [100%]	5 [100%]	5 [100%]
Kidney No lesions	2 [40%]	5 [100%]	5 [100%]
Nuclear debris in glomeruli and in blood vessels	3 [60%]	0 [0%]	0 [0%]
Liver			
No lesions	4 [80%]	4 [80%]	4 [80%]
Mild bile duct proliferation	0 [0%]	0 [0%]	1 [20%]
Few perivenular cells containing yellow refractile material	0 [0%]	1 [20%]	1 [20%]
Incidental finding: Bile pigment in few bile ducts	1 [20%]	0 [0%]	0 [0%]
Lungs No lesions]	5 [100%]	5 [100%]	5 [100%]
Lymph Node			
Populated by leukemia cells	5 [100%]	0 [0%]	0 [0%]
Occupied by stroma, few lymphocytes, and subcapsular macrophages	0 [0%]	5 [100%]	5 [100%]
Ovary			
No lesions	5 [100%]	5 [100%]	5 [100%]
Pancreas			
No lesions	5 [100%]	5 [100%]	5 [100%]
Sciatic Nerve			
No lesions	5 [100%]	5 [100%]	5 [100%]
Skeletal Muscle			
No lesions	4 [80%]	5 [100%]	5 [100%]

Incidental finding: Single necrotic cell	1 [20%]	0 [0%]	0 [0%]
Spinal Cord			
No lesions	4 [80%]	5 [100%]	5 [100%]
Meninges, few leukemia cells	1 [20%]	0 [0%]	0 [0%]
Thymus			
Populated by leukemia cells	5 [100%]	1 [20%]	0 [0%]
Populated by stroma and few lymphocytes	0 [0%]	1 [20%]	5 [100%]
Populated by mix of leukemia cells and lymphocytes	0 [0%]	3 [60%]	0 [0%]
Thyroid			
No lesions	5 [100%]	5 [100%]	4 [80%]
Incidental finding: Mild lymphocytic infiltrate into and near parathyroid	0 [0%]	0 [0%]	1 [20%]
Urinary Bladder			
No lesions	5 [100%]	5 [100%]	5 [100%]
Uterus			
No lesions	5 [100%]	5 [100%]	5 [100%]